Electronic Supplementary Material (ESI) for Polymer Chemistry.

Chemically recyclable fluorescent polyesters via the ring-opening copolymerization of epoxides and anhydrides

Taylor B. Young, Owaen G. Guppy, Alysia J. Draper, Joshua Whittington, Benson M. Kariuki, Alison Paul, Mark Eaton, Simon J. A. Pope,* Benjamin D. Ward *

Electronic supplementary information

Contents

S1. Experimental details and characterizing data

S1.1. General methods and instrumentation

Synthesis of luminophores were carried out using commercially available reagents without further purification. Catalyst reactions were carried out used a Radleys ReactorReady under an atmosphere of argon. Toluene was dried by passing through an alumina drying column incorporated into a MBraun SPS800 solvent purification system. Photophysical data were obtained on a JobinYvon-Horiba Fluorolog spectrometer fitted with a JY TBX picosecond photodetection module as chloroform solutions. Emission spectra were uncorrected and excitation spectra were instrument corrected. The pulsed source was a Nano-LED configured with for a 295 nm output at 1 MHz. Luminescence lifetimes were obtained using the JobinYvon-Horiba FluoroHub single photon counting module fitting the lifetime data using DAS6 deconvolution software. Quantum yield measurements were obtained on aerated solutions using $[Ru(bipy)_3](PF_6)_2$ in MeCN ($\phi = 0.016$) or quinine sulfate in 0.05 M H_2SO_4 as standards ($\phi = 0.60$). For the measurement of ^1H, and ^{13}C NMR spectra a Bruker Fourier300 (300 MHz), Bruker AVANCE HD III equipped with a BFFO SmartProbe™ (400 MHz) or Bruker AVANCE III HD with BBO Prodigy CryoProbe (500 MHz) was used. The obtained chemical shifts δ are reported in ppm and are referenced to the residual solvent signal. Spin–spin coupling constants J are given in Hz. UV-Visible spectroscopy was performed in aerated chloroform solutions using a Shimadzu UV-1800 spectrophotometer. IR spectra were recorded on an ATR equipped Shimadzu IRAffinity-1 spectrophotometer. GPC data were measured on an Agilent 1260 II triple-detection GPC system. Molecular weights were measured using 3 mg of polymer dissolved in 1 ML THF at 30 °C using a THF mobile phase with flow rate of 1 mL min^{-1}. Calibration of the triple detection was performed with a polystyrene standard with dn/dc of 0.185 g/mL. Thermal properties were measured using a double furnace, power compensation DSC 8000 (Perkin Elmer, UK). The DSC was calibrated using indium and an empty sealed sample pan was used as a reference. Samples were heated from -50°C to 180 °C, at a rate of 30 °C min^{-1}, under nitrogen flow, followed by an isothermal hold at 150 °C for 1 min. The samples were then cooled to -50 °C, at a rate of 30 °C min^{-1}, and kept at -50 °C for a further 1 min. Each sample was run for three heating–cooling cycles. The reported glass transition temperatures (Tg) were taken from the third heating cycles.

S1.2 Syntheses of pre-catalyst and monomers

S1.2.1. [Al(^{t}Bu-Salen)Cl] (3): Synthesized according to previous literature methods.[1] ^{t}Bu-Salen-H_2 (1.00 g, 2.03 mmol) was dissolved in toluene and diethylaluminium chloride (2.03 mL, 2.03 mmol, 1 M solution in toluene) was added dropwise, and the reaction allowed to stir at room temperature for an hour. Afterwards the solvent was removed, washed with hexane, and dried *in vacuo* to furnish the desired compound as a yellow solid (1.05 g, 93%). ^1H NMR (300 MHz, $CDCl_3$) δ 8.31 (2 H, s, CH), 7.49 (2 H, d, J = 2.59, CH), 6.98 (2 H, d, J = 2.58, CH) 4.17 – 3.98 (2 H, m, CH_2), 3.79 – 3.57 (2 H, m, CH_2), 1.47 (9 H, s, CH_3), 1.23 (9 H, s, CH_3). UV-Vis ($CHCl_3$) λ_{max} (ε / $dm^3mol^{-1}cm^{-1}$): 364 (11459), 280sh (27513), 291 (29419) nm. Emission ($CHCl_3$): λ_{em} (τ/ns) = 480 (10.45) nm.

S1.2.2. 4-Piperidinyl-(N-propylene-oxide)-1,8-naphthalimide (Nap, 1): Synthesized using a published procedure;[2] the structure was verified by X-ray diffraction analysis as provided in S2.2. 4-piperidinyl-1,8-naphthalimide (1.00 g, 3.57 mmol) and potassium carbonate (0.493 g, 3.57 mmol) were added to epichlorohydrin (20 mL) and heated at reflux for five hours. After which, the reaction was allowed to cool, filtered, washed with dichloromethane, and the solvent removed. The resulting orange powder was recrystallized from ethanol to give the **Nap** as orange needles (0.960 g, 80%). ^{1}H NMR (500 MHz, $CDCl_3$) δ 8.59 (1 H, dd, J = 7.3, 1.2 Hz, CH), 8.51 (1 H, d, J = 8.1 Hz, CH), 8.40 (1 H, dd, J = 8.4, 1.2 Hz, CH), 7.68 (1 H, dd, J = 8.4, 7.3 Hz, CH), 7.18 (1 H, d, J = 8.1 Hz, CH), 4.52 (1 H, dd, J = 13.5, 4.9 Hz, CH), 4.26 (1 H, dd, J = 13.5, 5.4 Hz, CH), 3.39 – 3.31 (1 H, m), 3.29 – 3.20 (4 H, m, CH_2), 2.82 – 2.77 (2 H, m, CH_2), 1.93 – 1.84 (4 H, m, CH2), 1.78 – 1.69 (2 H, m, CH2). ^{13}C{^{1}H} NMR (126 MHz, $CDCl_3$) δ 164.82, 164.27, 157.73, 133.15, 131.47, 131.07, 130.24, 126.45, 125.53, 123.00, 115.69, 114.90, 77.16, 54.70, 49.56, 46.77, 41.74, 26.37, 24.49. HRMS (ESI+) calcd for $C_{20}H_{21}N_2O_3$: 337.1552 $[M+H]^+$, found: 337.1551. Ir ν_{max}/cm-1 (neat): 3076, 2980, 2957, 2838, 2918, 2845, 2794, 1690 (C=O), 1651 (C=O) , 1587, 1574, 1518, 1457, 1448, 1429, 1406, 1396, 1373, 1341, 1317, 1256, 1234, 1223, 1186, 1157, 1134, 1115, 1082, 1062, 1028, 981, 963, 914, 898, 864, 846, 839, 829, 785, 771, 754, 734, 699, 652, 604, 588, 530, 502, 476, 462, 419. UV-Vis ($CHCl_3$) λ_{max} (ε / $dm^3mol^{-1}cm^{-1}$): 413 (10321), 342 (2294), 327 (1988), 280 (11846) nm. Emission ($CHCl_3$): λ_{em} (τ/ns) = 510 (8.90) nm.

S1.2.3. 1-(3-chloro-2-hydroxypropyl)aminoanthraquinone (intermediate for AAQ, 2): Synthesized using a published procedure.[3] 1-aminoanthraquinone (2.00 g, 8.96 mmol) was dissolved in epichlorohydrin (14 mL, 179.19 mmol) with acetic acid (2.05 mL, 35.84 mmol)) and heated at 80 °C for 25 hours. After cooling a dark purple precipitate was collected on a glass sinter and washed with ice cold IPA and dried to afford the title compound as fluffy burgundy crystals (2.243 g, 80%). ^{1}H NMR (500 MHz, $CDCl_3$) δ 9.95 (1 H, s, NH), 8.28 (1H, d, J = 7.26 Hz, CH), 8.24 (1 H, d, J = 7.58, CH), 7.77 (1H, td, J = 7.44, 1.10 Hz, CH), 7.72 (1 H, td, J = 7.45, 1.03, CH), 7.64 (1 H, d, J = 7.27 Hz, CH), 7.57 (1 H, t, J = 7.95, CH), 7.13 (1 H, d, J = 8.52 Hz, CH), 4.25 – 4.15 (1 H, m, CH), 3.74 (2 H, qd, J = 11.32, 5.31, CH_2), 3.67 – 3.59 (1 H, m, CH_2), 3.57 – 3.49 (1H, m, CH_2), 2.67 (1 H, d, J = 5.2 Hz, OH). ^{13}C{^{1}H} NMR (126 MHz, $CDCl_3$) δ 185.53, 183.31, 151.68, 135.64, 134.96, 134.90, 134.20, 133.32, 133.11, 126.94, 126.93, 117.88, 116.47, 113.76, 70.11, 47.63, 45.93. HRMS (ESI+) calcd for $C_{17}H_{14}ClNO_3$: 316.0740 $[M+H]^+$, found 316.0736. IR ν_{max}/cm^{-1} (neat): 3422 (OH), 3271 (NH), 3065, 1667 (C=O), 1620 (C=O), 1587, 1560, 1501, 1458, 1424, 1416, 1387, 1313, 1302, 1267, 1236, 1201, 1171, 1159, 1130, 1072, 1058, 999, 987, 908, 891, 858, 804, 777, 735, 704, 675, 644, 609, 588, 546, 494, 474, 465, 419. UV-Vis ($CHCl_3$) λ_{max} (ε / $dm^3mol^{-1}cm^{-1}$): 497 (7104), 314 (6619), 283sh (10310), 275 (11537) nm. Emission ($CHCl_3$): λ_{em} (τ/ns) = 590 (<1 ns) nm.

S1.2.4. 1-(propylene-oxide)aminoanthraquinone (AAQ, 2): The structure was verified by X-ray diffraction analysis as provided in S2.3. 1-((3-chloro-2-hydroxypropyl)aminoanthraquinone (1.25 g, 3.96 mmol) was dissolved in dioxane (13 mL) along with powdered potassium hydroxide (0.777 g, 13.86 mmol) and stirred at room temperature for 2 hours. After which the mixture was extracted with DCM, washed with water, brine, dried over magnesium sulfate, filtered and the solvent removed *in vacuo* to afford **AAQ** as a bright red solid (0.925 g, 84 %). ^{1}H NMR (500 MHz, $CDCl_3$) δ 9.87 (1 H, s, NH), 8.29 (1 H, ddd, J = 7.75, 1.41, 0.52, CH), 8.25 (1 H,

ddd, J = 7.58, 1.47, 0.52, CH), 7.77 (1 H, td, J = 7.33, 1.43 Hz, CH), 7.72 (1H, td, J = 7.43, 1.43 Hz, 1H), 7.65 (1 H, dd, J = 7.37, 1.15 Hz, CH), 7.58 (1 H, J = 8.55, 7.38, CH), 7.17 (1 H, dd, J = 8.56, 1.13 Hz, CH), 3.75 (1H, dt, J = 14.79, 3.43 Hz, CH_2) 3.54 (1H, dt, J = 14.62, 4.54 Hz, CH_2) 3.28 (1 H, dddd, J = 4.76, 3.93, 3.42, 2.66 Hz, CH), 2.88 (1H,dd, J = 4.76, 3.98 Hz, CH_2), 2.75 (1 H, dd, J = 4.79, 2.64 Hz, CH_2). $^{13}C\{^1H\}$ NMR (126 MHz, $CDCl_3$) δ = 185.48, 183.87, 151.85, 135.57, 135.01, 134.83, 134.17, 133.28, 133.15, 126.95, 126.92, 118.16, 116.47, 113.65, 77.16, 50.92, 45.30, 44.27. HRMS (ESI+) calcd for $C_{17}H_{14}NO_3$: 280.0974 $[M+H]^+$ found 280.0963. IR ν_{max}/cm^{-1} (neat): 3259 (NH), 3070, 2993, 1661 (C=O), 1628 (C=O), 1593, 1570, 1508, 1367, 1302, 1269, 1230, 1175, 1157, 1141, 1072, 997, 957, 919, 829, 708, 330, 547, 419, 411. UV-Vis ($CHCl_3$) λ_{max} (ε / $dm^3mol^{-1}cm^{-1}$): 497 (8029), 315 (7586), 284sh (12684), 274 (14170) nm. Emission ($CHCl_3$): λ_{em} (τ/ns) = 588 (<1 ns) nm.

S1.3. Polymer syntheses

S1.3.1. Polymer synthesis:

Large scale: A Radleys ReactorReady fitted with a 2 l vessel, mechanical stirrer, bubbler, inert gas inlet valve, and a thermocouple (see image below), was purged with argon for 20 minutes. Phthalic anhydride (189.50 g, 1280 mmol), cyclohexene oxide (130 mL, 1277 mmol), toluene (500 mL), [Al(Salen)Cl] (**1**) (1.75 g, 3.16 mmol), and dimethylaminopyridine (0.78 g, 6.38 mmol) were added to one of the access ports under a positive flow of argon, and the vessel heated to 80 °C (using an internal thermocouple) for 3 days with stirring at 400 rpm. Conversion was determined using ^1H NMR spectroscopy by integrating the phthalic anhydride signals and the corresponding signals in the polymer. After cooling to 50 °C, the mixture was poured into methanol (1000 mL) and the resulting precipitate allowed to settle, before the solvent was decanted. Isopropanol (800 mL) was added to the precipitate, stirred and the polymer allowed to settle before decanting the liquid and repeating the process a further three times. The precipitated polymer was collected on a glass sinter and dried with suction. The polymer was further dried in a vacuum oven at 80 °C overnight.

Small scale: A 7 mL screw cap vial was charged in a glove box. Anhydride (400 eq), epoxide (400 eq), toluene (1 mL), [Al(Salen)Cl] (**1**) (3.5 mg, 6.4 µmol), and dimethylaminopyridine (2 eq) were added sequentially. The vial was closed and heated to 80 °C on an aluminium heating block. A blank vial containing 1 mL of paraffin oil was used for the thermocouple to ensure an accurate temperature reading). The reaction was stirred for 48 hours. The mixture was poured into methanol (30 mL) and the resulting precipitate allowed to settle, before the solvent was decanted. The precipitated polymer was collected on a glass sinter and dried with suction. The polymer was further dried in a vacuum oven at 80 °C overnight.

The alternating microstructure was determined by integration of the ester and ether signals in the ^1H NMR spectra and are shown below.[4]

S1.3.2. Undoped Polymer (PA-CHO): Yield 310 g. ^{1}H NMR (500 MHz, $CDCl_3$) δ 7.64 – 7.53 (2 H, Br. m CH), 7.46 – 7.33 (2 H, Br. m, CH), 5.26 – 5.06 (2 H, Br. m, CH), 2.29 – 2.13 (2 H, Br. m, CH_2), 1.84 – 1.65 (2 H, Br. m, CH_2), 1.62 – 1.45 (2 H, Br. m, CH_2), 1.42 – 1.17 (2H, Br. m, CH_2). ($CHCl_3$) λ_{max} (ε / $dm^3mol^{-1}cm^{-1}$): 283sh (67315), 277 (73741) nm. Emission ($CHCl_3$): λ_{em} (τ/ns) = 482 (10.73) nm. M.p. 152-166 °C.

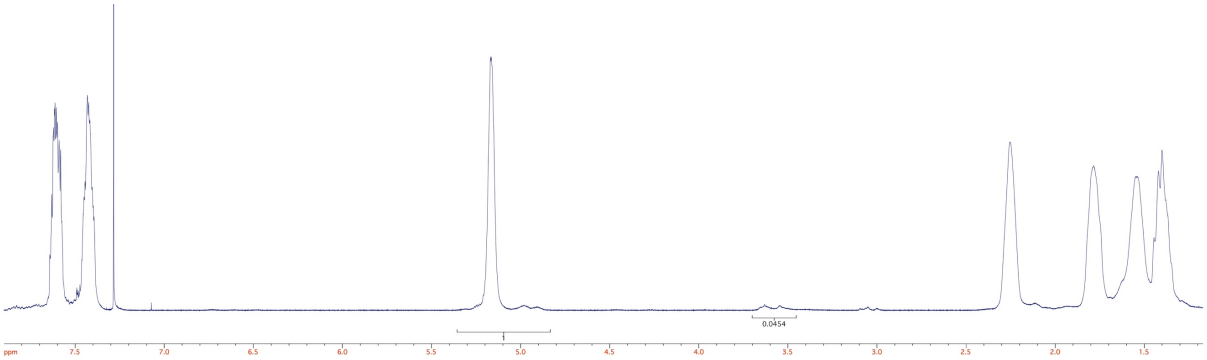

^{1}H NMR spectrum of PA-CHO (500 MHz, $CDCl_3$)

S1.3.3. Naphthalimide doped polymer (0.2% Nap-PA-CHO): Synthesized according to the general procedure but with the addition of 4-Piperidinyl-(N-propylene-oxide)-1,8-naphthalimide (Nap) (0.850 g, 2.53 mmol) as the dopant to yield Nap-PA-CHO as a bright yellow/green powder (320 g). ^{1}H NMR (500 MHz, $CDCl_3$) δ 7.64 – 7.53 (2 H, Br. m, CH), 7.45 – 7.34 (2 H, Br. m CH), 5.21 – 5.04 (2 H, Br. m, CH), 2.30 – 2.16 (2 H, Br. m, CH_2), 1.84 – 1.68 (2 H, Br. m, CH_2), 1.60 – 1.45 (2 H, Br. m, CH_2), 1.44 – 1.31 (2 H, Br. m, CH_2). UV-Vis ($CHCl_3$) λ_{max} (ε / $dm^3mol^{-1}cm^{-1}$): 411 (11639), 343 (3249), 327 (2772) nm. Emission ($CHCl_3$): λ_{em} (τ/ns) = 510 (8.88) nm. M.p. 152-166 °C.

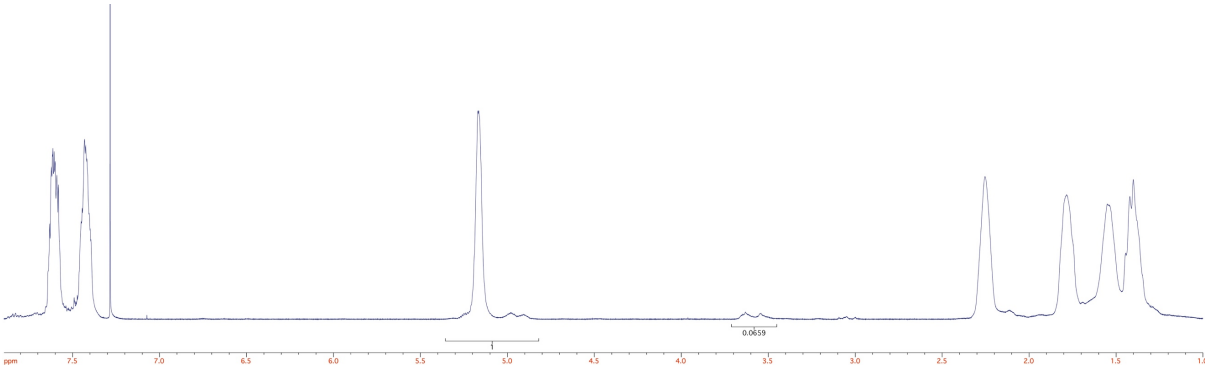

^{1}H NMR spectrum of Nap-PA-CHO (500 MHz, $CDCl_3$)

S1.3.4. Aminoanthraquinone doped polymer (0.2% AAQ-PA-CHO): Synthesized according to the general procedure but with the addition of 1-(propylene-oxide)aminoanthraquinone (0.706 g, 2.53 mmol) as the dopant to yield AAQ-PA-CHO as a light red solid (280 g). ^{1}H NMR (500 MHz, $CDCl_3$) δ 7.64 – 7.53 (2 H, Br. m, CH), 7.45 – 7.34 (2 H, Br. m, CH), 5.23 – 5.04 (2 H, Br. m, CH), 2.31 – 2.15 (2 H, Br. m, CH_2), 1.86 – 1.68 (2 H, Br. m, CH_2), 1.85 – 1.67 (2 H, Br. m, CH_2), 1.46 – 1.25 (2H, Br. m, CH_2). UV-Vis ($CHCl_3$) λ_{max} (ε / $dm^3mol^{-1}cm^{-1}$): 493 (13262), 360 (9126) nm. Emission ($CHCl_3$): λ_{em} (τ/ns) =584 (<1 ns) nm. M.p. 152-166 °C.

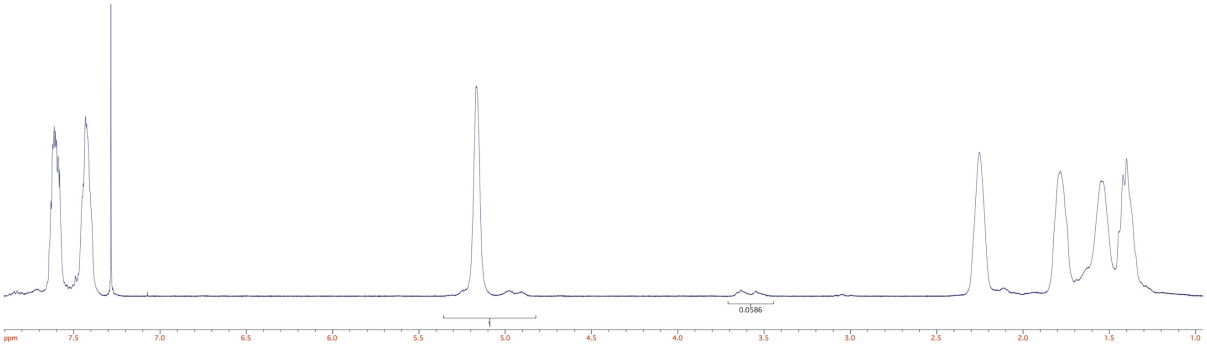

^{1}H NMR spectrum of AAQ-PA-CHO (500 MHz, $CDCl_3$)

S1.3.5 Top to Bottom: 12%, 33%, 63% Nap-PA-CHO (Table 1: Entries 3, 4, 5 respectively).

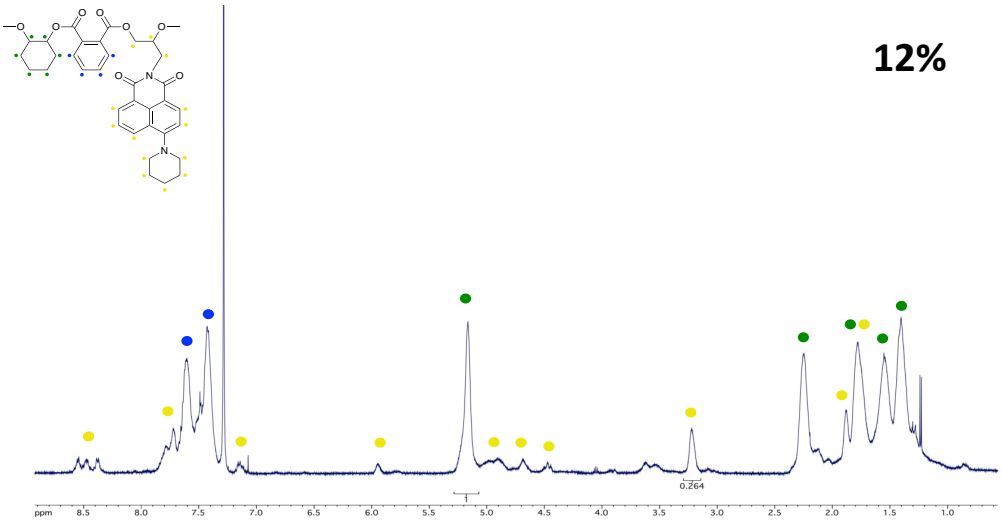

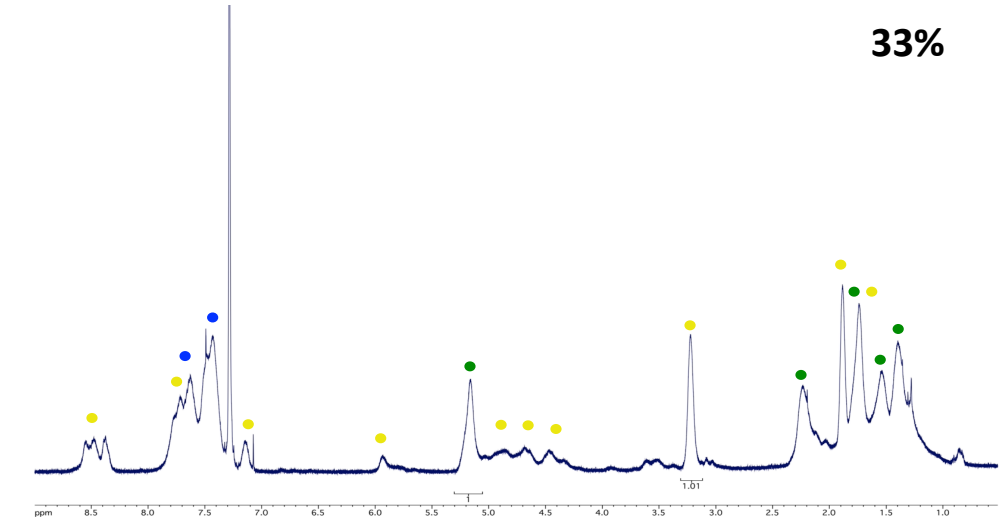

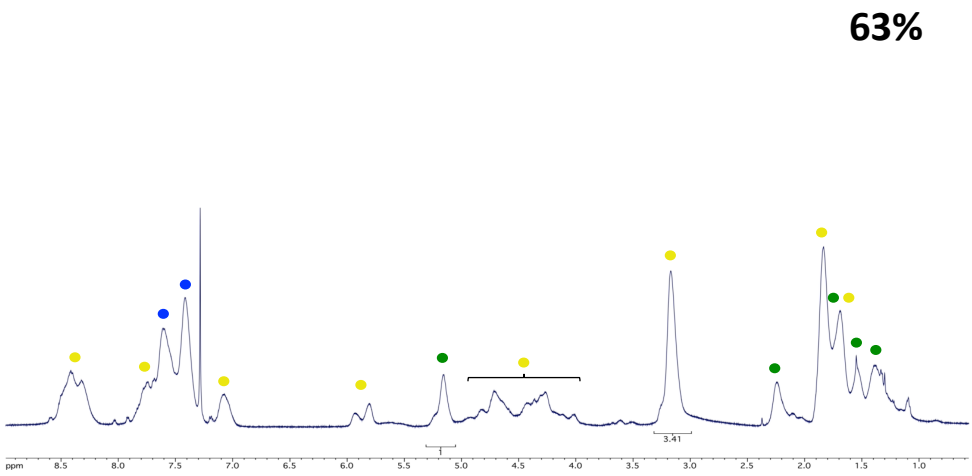

S1.3.5.1 Incorporation Calculation Example – 12% NAP-PA-CHO

The signal at 5.1 ppm corresponds to two CH protons (2H) adjacent to the ester linkage, associated with CHO (•). The signal at 3.1 ppm corresponds to two CH_2 protons (4H) adjacent to the tertiary amine of the piperidine ring on the NAP unit (•). This resonance was selected for incorporation calculation as it afforded minimal overlap with other peaks across all dopant concentrations. Incorporation of the NAP monomer was calculated by comparing the integrations of the signals above, taking into account the relative number of protons giving rise to each signal, e.g. in the example below, (0.264/2)/(1+ (0.264/2))x100 = 12%

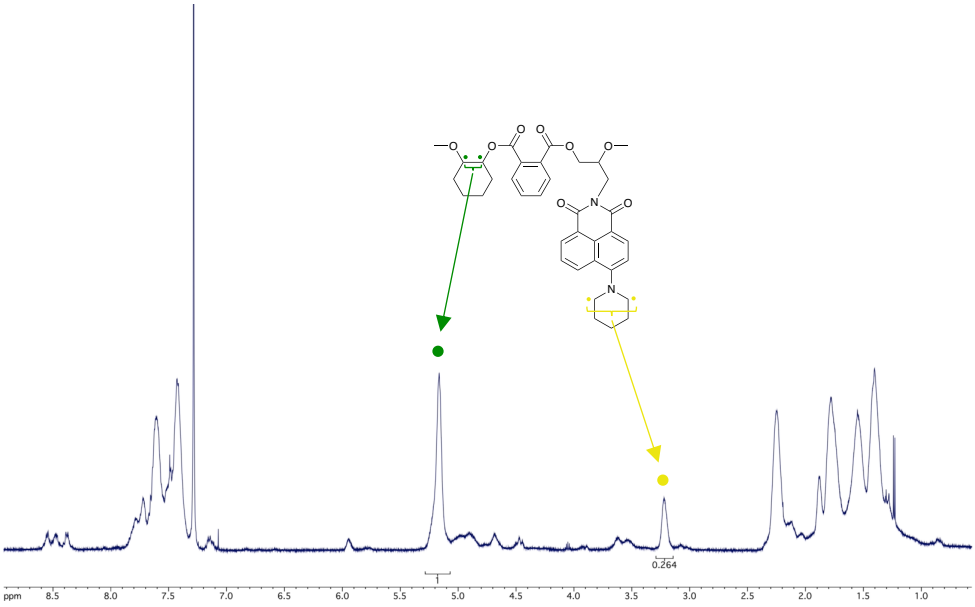

S1.3.6 Top to Bottom: 14%, 34%, 64% AAQ-PA-CHO (Table 1: Entries 7, 8, 9 respectively).

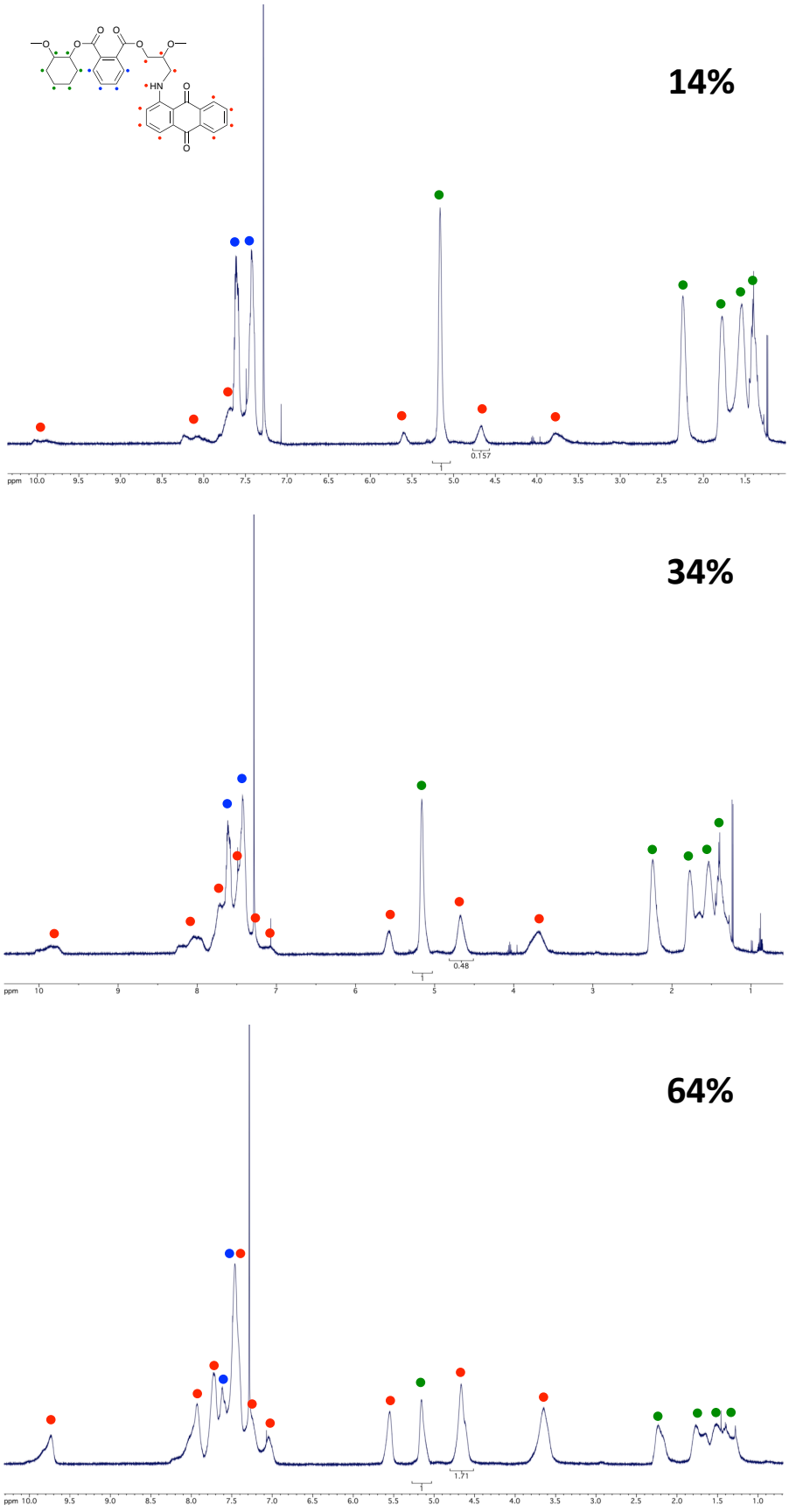

S1.3.6.1 Incorporation Calculation Example – 14% AAQ-PA-CHO

The signal at 5.1 ppm corresponds to two CH protons (2H) adjacent to the ester linkage, associated with CHO (•). The signal at 4.7 ppm corresponds to the CH_2 (2H) adjacent to the secondary amine of the AAQ unit (•). Incorporation of the AAQ monomer was calculated by comparing the integrations of these two signals, e.g. in the example below, 0.157/(1+0.157)x100 = 14%.

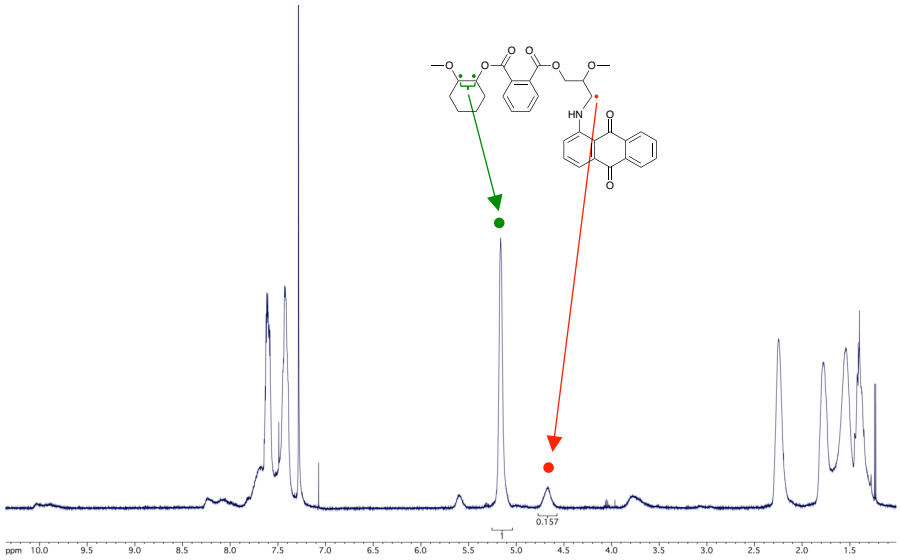

S1.3.7 TPhA-CHO – Entry 10

^{1}H NMR (500 MHz, $CDCl_3$) δ 5.01 (Br. m, 2H, CH), 2.04 (Br. m, 2H, CH), 1.54 (Br. m, 4H, CH), 1.32 (Br. m, 2H, CH).

S1.3.8 PA-PO – Entry 11

^{1}H NMR (500 MHz, $CDCl_3$) δ 7.63 (Br. m, 1H, CH), 7.59 (Br. m, 1H, CH), 7.41 (Br. m, 2H, CH), 5.34 (Br. m, 1H, CH), 4.32 (Br. m, 2H, CH2), 1.29 (Br. m, 3H, CH3).

S1.3.9 Nap-TPhA-CHO – Entry 12

^{1}H NMR (500 MHz, $CDCl_3$) δ 5.08 (Br. m, 2H, CH), 2.12 (Br. m, 2H, CH_2), 1.62 (Br. m, 4H, CH_2), 1.37 (Br. m, 2H, CH_2).

S1.3.10 Nap-PA-PO – Entry 13

^{1}H NMR (500 MHz, $CDCl_3$) δ 7.61 (Br. m, 2H, CH), 7.41 (Br. m, 2H, CH), 5.34 (Br. m, 1H, CH), 4.31 (Br. m, 2H, CH_2), 1.29 (Br. m, 3H, CH_3).

S1.3.11 AAQ-TPhA-CHO – Entry 14

^{1}H NMR (500 MHz, $CDCl_3$) δ 5.01 (Br. m, 2H, CH), 2.02 (Br. m, 2H, CH_2), 1.60 (Br. m, 4H, CH_2), 1.31 (Br. m, 2H, CH_2).

S1.3.12 AAQ-PA-PO – Entry 15

^{1}H NMR (500 MHz, $CDCl_3$) δ 7.51 (Br. m, 4H, CH), 5.33 (Br. m, 1H, CH), 4.32 (Br. m, 2H, CH_2), 1.27 (Br. m, 3H, CH_3).

S1.3.13 Recycled Polymer – Entry 16

^{1}H NMR (500 MHz, $CDCl_3$) δ 7.50 (Br. m, 2H, CH), 7.38 (Br. m, 2H, CH), 5.11 (Br. m, 2H, CH), 2.16 (Br. m, 2H, CH_2), 1.65 (Br. m, 2H, CH_2), 1.49 (Br. m, 2H, CH_2), 1.32 (Br. m, 2H, CH_2).

S1.4 Percentage Ester Calculation Examples

Selectivity (percentage ester) was calculated by comparing the integrations of ether to ester signals. The table below gives the clearest and most distinct signals that we have used in our calculations:

Epoxide	**Ester signals / ppm**	**Ether signals / ppm**
CHO	5.1-5.2 (2 CH)	3.2-3.6
PO	5.4-5.5 (CH)	3.0-3.1
Nap	5.9-6.0 (CH) [a]	3.0-3.1
AAQ	5.5-5.6 (CH) [a]	2.9-3.0

[a] These integration value should be multiplied by 2 before comparing with CHO integration owing to the different number of protons associated with the signals.

Cyclohexene Oxide Example - PA-CHO (Entry 1)

As seen below, ether peaks for CHO[5] are present at 3.5-3.7 ppm and the ester peak at 5.6-5.7 ppm. Each peak represents two protons, by comparing the integrations percentage ester can be calculated e.g. (1/1+0.0454)x100=96%.

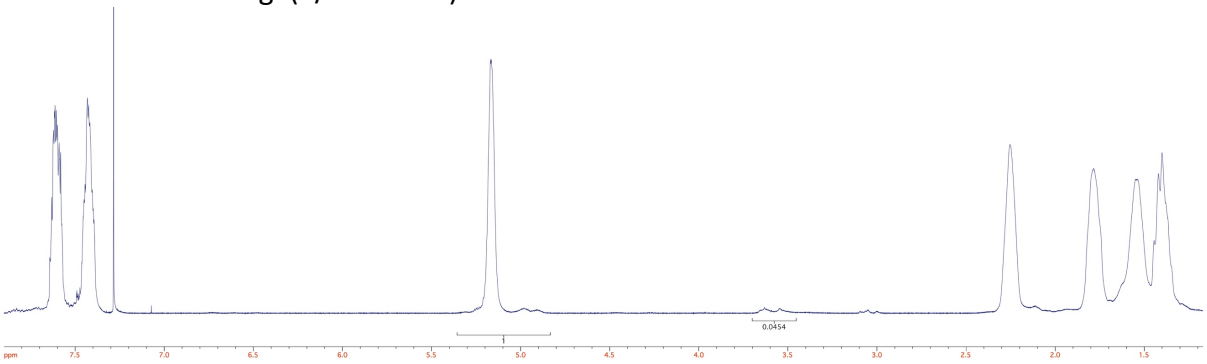

^{1}H NMR spectrum of PA-CHO (500 MHz, $CDCl_3$)

Propylene Oxide Example - PA-PO (Entry 11)

Ether peaks for PO[6] are present below at 3.1-3.2 ppm and the ester peak is present at 5.4-5.5 ppm. The ester peak represents two protons and the ether peaks represents 3 protons. by comparing the integrations, percentage ester can be calculated e.g. (0.5)/0.5+(0.0696/3))x100=95%.

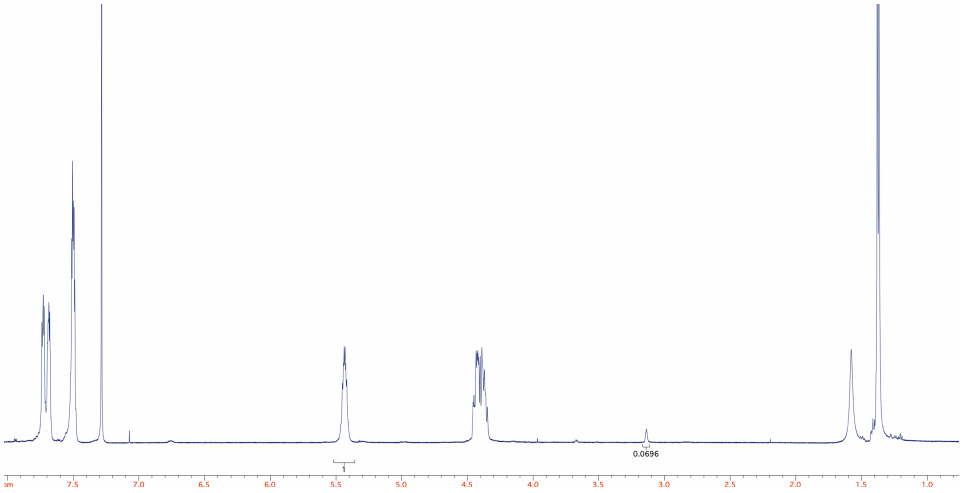

^{1}H NMR spectrum of PA-PO (500 MHz, $CDCl_3$)

Propylene Oxide Example – Nap-PA-PO (33%, Entry 4)
Similar to above examples, but ester and ether regions now from both epoxide monomers, e.g. in the example below, ((0.0944x2)+0.764)/1.075))x100=89%.

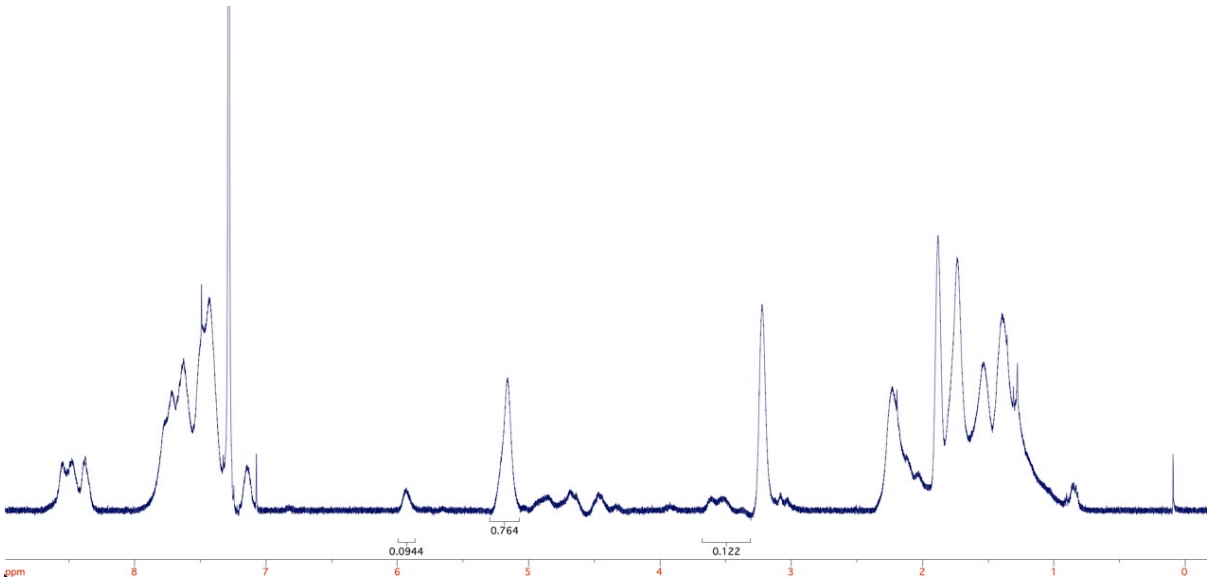

S2. X-ray data

S2.1. Experimental details

Single crystals of the two chromophore monomers **2** and **3** were grown by the slow diffusion of petroleum ether into dichloromethane solutions at room temperature. Single-crystal X-ray diffraction data (Mo-Kα) were collected on a Rigaku Saturn 724+ CCD diffractometer at low temperature, by the EPSRC National Crystallographic Service.[7] Single crystals of *trans*-1,2-cyclohexanediol were grown by the slow evaporation of an ethyl acetate solution and X-ray data (Cu-Kα) collected on an Agilent Supernova CCD diffractometer in the Cardiff School of Chemistry. Crystal structures were solved using direct methods with absorption corrections being applied as part of the data reduction scaling procedure. After refinement of the heavy atoms, difference Fourier maps revealed the maxima of residual electron density close to the positions expected for the hydrogen atoms; they were introduced as fixed contributors in the structure factor calculations and treated with a riding model, with isotropic atomic displacement parameters but not refined. Full least-square refinement was carried out on F^2. A final difference Fourier map revealed no significant maxima or minima of residual electron density. The scattering factor coefficients and the anomalous dispersion coefficients were taken from standard sources. Crystal structures were solved using SHELXT and refined using SHELXL-2013 via the Olex2 program.[8–11] Crystallographic data and experimental details are given in S2.2-4. The epoxide group was found to be disordered for both **2** and **3**, and was modelled over two sites. In **3**, the N-H position was located in the Fourier difference map and its position refined with the N-H distance restrained to 0.88 Å and U_{iso} fixed at 1.2 U_{eq}(N). CCDC numbers 2094967-2094969.

S2.2. Naphthalimide monomer (1)

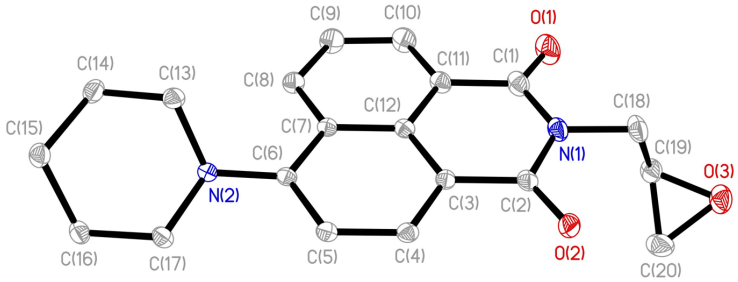

Crystal data and structure refinement for 2.

Identification code	og5	
Empirical formula	$C_{20}H_{20}N_2O_3$	
Formula weight	336.38	
Temperature	100(2) K	
Wavelength	0.71073 Å	
Crystal system	Orthorhombic	
Space group	Pbca	
Unit cell dimensions	*a* = 12.782(3) Å	a = 90 °
	b = 7.6564(15) Å	b = 90 °
	c = 32.715(7) Å	g = 90 °
Volume	3201.5(11) Å^3	

Z	8
Density (calculated)	1.396 Mg/m^3
Absorption coefficient	0.095 mm^{-1}
F(000)	1424
Crystal size	0.180 × 0.080 × 0.020 mm^3
θ range for data collection	2.022 to 32.669 °
Index ranges	–14 ≤ h ≤ 19, –10 ≤ k ≤ 9, –47 ≤ l ≤ 47
Reflections collected	43523
Independent reflections	5218 [R(int) = 0.0280]
Completeness to θ = 25.242 °	100.0%
Absorption correction	Semi-empirical from equivalents
Max. and min. transmission	1.00000 and 0.82305
Refinement method	Full-matrix least-squares on F^2
Data / restraints / parameters	5218 / 138 / 263
Goodness-of-fit on F^2	1.187
Final R indices [I>2σ(I)]	R_1 = 0.0764, wR_2 = 0.2052
R indices (all data)	R_1 = 0.0870, wR_2 = 0.2115
Extinction coefficient	n/a
Largest diff. peak and hole	0.485 and -0.423 e.Å^{-3}

S2.3. Aminoquinoline monomer (2)

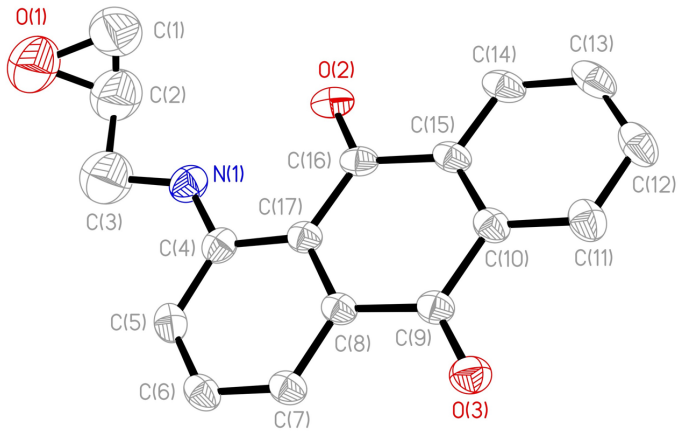

Crystal data and structure refinement for 3.

Identification code	og4
Empirical formula	$C_{17}H_{13}NO_3$
Formula weight	279.28
Temperature	100(2) K
Wavelength	0.71073 Å
Crystal system	Trigonal
Space group	$R\bar{3}$

Unit cell dimensions	*a* = 29.6286(6) Å	a = 90 °
	b = 29.6286(6) Å	b = 90 °
	c = 7.6747(3) Å	g = 120 °
Volume	5834.6(3) Å^3	
Z	18	
Density (calculated)	1.431 Mg/m^3	
Absorption coefficient	0.099 mm^{-1}	
F(000)	2628	
Crystal size	0.300 × 0.058 × 0.020 mm^3	
θ range for data collection	2.381 to 27.481 °	
Index ranges	–38 ≤ h ≤ 38, –38 ≤ k ≤ 38, –9 ≤ l ≤ 9	
Reflections collected	33544	
Independent reflections	2976 [R(int) = 0.0710]	
Completeness to θ = 25.242 °	100.0%	
Absorption correction	Gaussian	
Max. and min. transmission	1.000 and 0.792	
Refinement method	Full-matrix least-squares on F^2	
Data / restraints / parameters	2976 / 103 / 230	
Goodness-of-fit on F^2	1.063	
Final R indices [I>2σ(I)]	R_1 = 0.0668, wR_2 = 0.2022	
R indices (all data)	R_1 = 0.0799, wR_2 = 0.2181	
Extinction coefficient	n/a	
Largest diff. peak and hole	0.316 and -0.332 e.Å^{-3}	

S2.4. 1,2-cyclohexane-diol

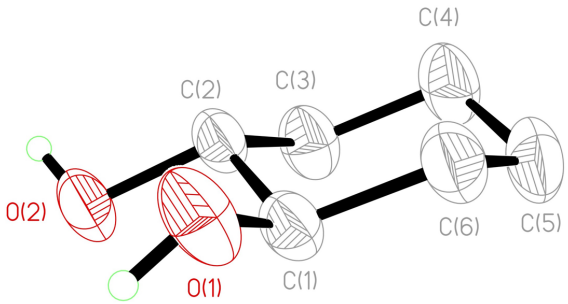

Crystal data and structure refinement for 1,2-cyclohexane-diol.

Identification code	tby1
Empirical formula	$C_6H_{12}O_2$
Formula weight	116.16
Temperature	296 K
Wavelength	1.54184 Å

Crystal system	Monoclinic	
Space group	C2/c	
Unit cell dimensions	a = 18.6396(18) Å	a = 90 °
	b = 9.9559(7) Å	b = 96.583(7) °
	c = 7.3000(6) Å	g = 90 °
Volume	1345.8(2) $Å^3$	
Z	8	
Density (calculated)	1.147 Mg/m^3	
Absorption coefficient	0.687 mm^{-1}	
F(000)	512	
Crystal size	0.306 × 0.113 × 0.107 mm^3	
θ range for data collection	4.776 to 76.481 °	
Index ranges	–21 ≤ h ≤ 23, –12 ≤ k ≤ 12, –9 ≤ l ≤ 9	
Reflections collected	6179	
Independent reflections	1412 [R(int) = 0.0164]	
Completeness to θ = 67.684 °	100.0%	
Absorption correction	Gaussian	
Max. and min. transmission	1.000 and 0.607	
Refinement method	Full-matrix least-squares on F^2	
Data / restraints / parameters	1412 / 316 / 150	
Goodness-of-fit on F^2	1.064	
Final R indices [I>2σ(I)]	R_1 = 0.0397, wR_2 = 0.1183	
R indices (all data)	R_1 = 0.0472, wR_2 = 0.1275	
Extinction coefficient	n/a	
Largest diff. peak and hole	0.090 and -0.118 e.$Å^{-3}$	

S3. GPC, DOSY, and DSC data

S3.1. GPC traces of polymers

S3.1.1. GPC trace of PA-CHO

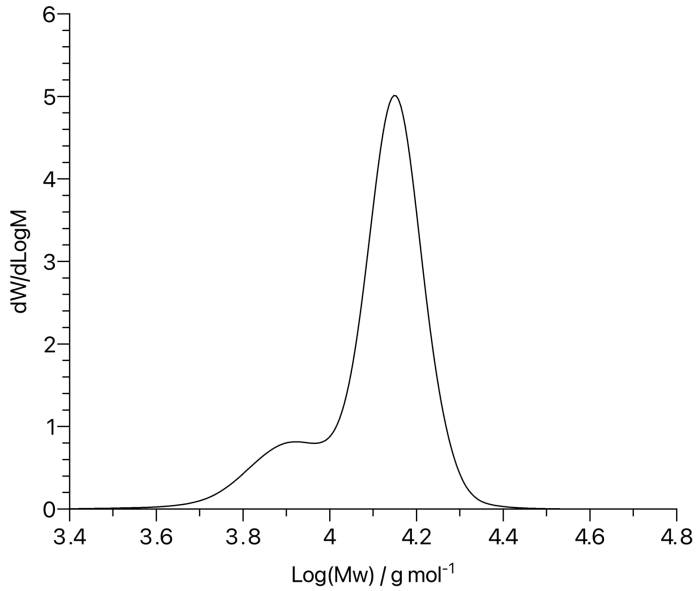

S3.1.2. GPC trace of 0.2% Nap-PA-CHO

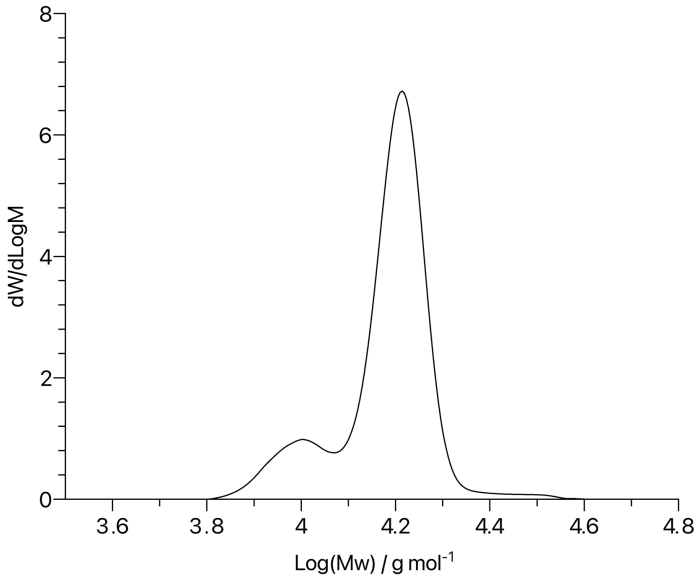

S3.1.3. GPC trace of 12% Nap-PA-CHO

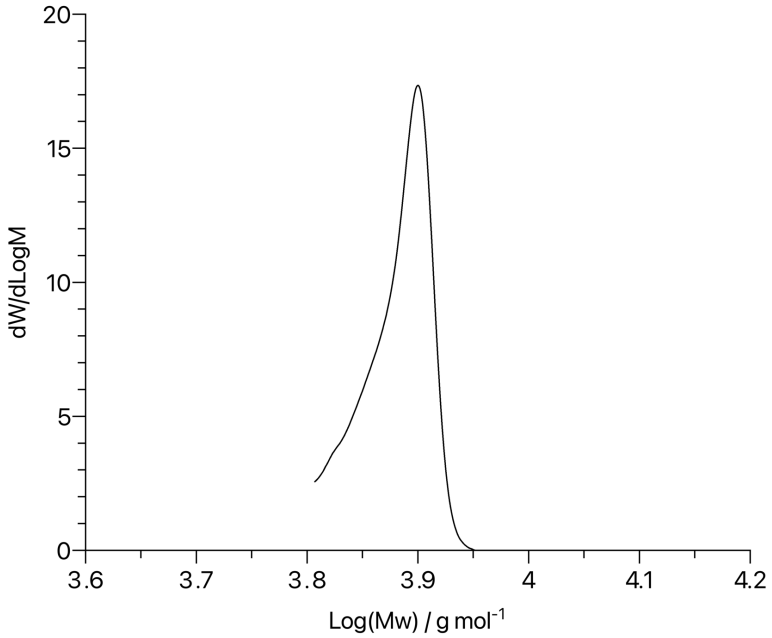

S3.1.4. GPC trace of 33% Nap-PA-CHO

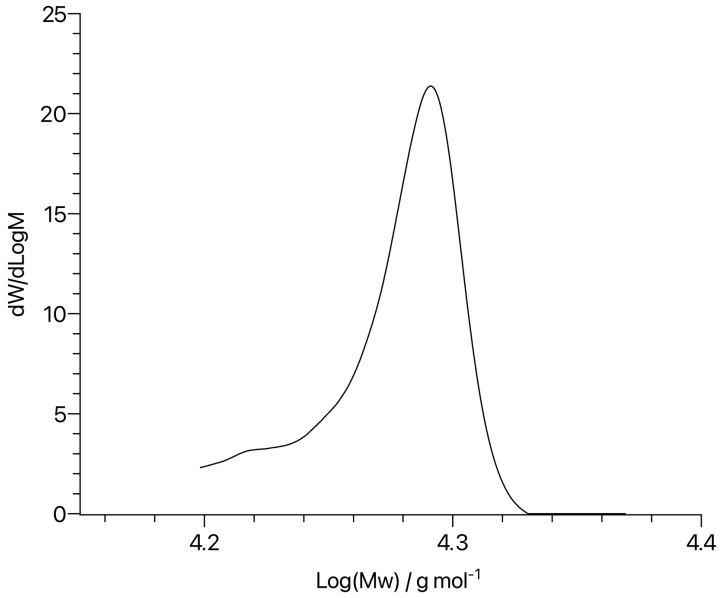

S3.1.5. GPC trace of 63% Nap-PA-CHO

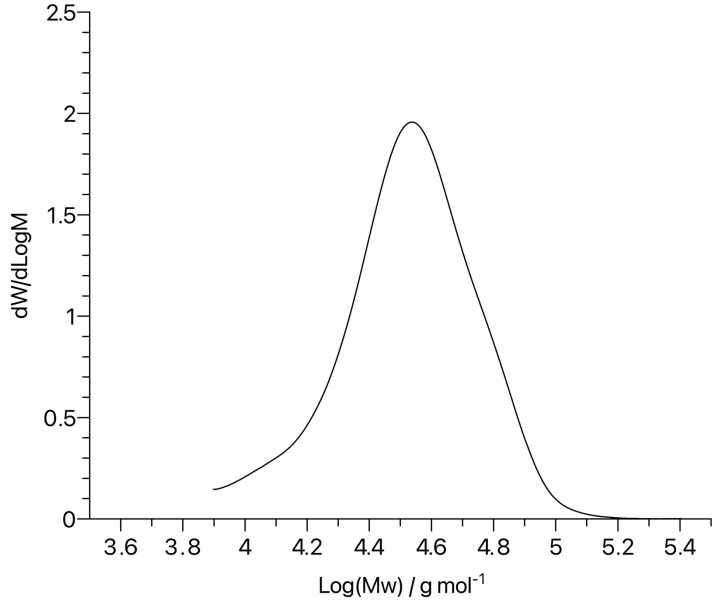

S3.1.6. GPC trace of 0.2% AAQ-PA-CHO

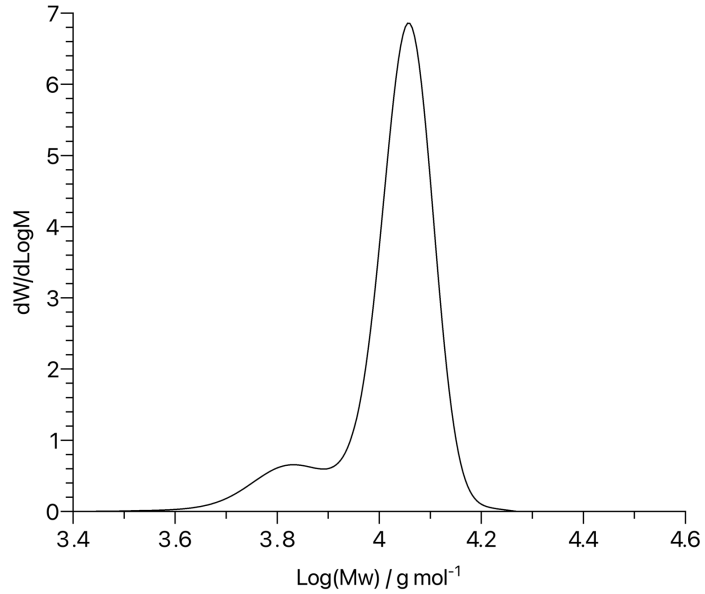

S3.1.7. GPC trace of 14% AAQ-PA-CHO

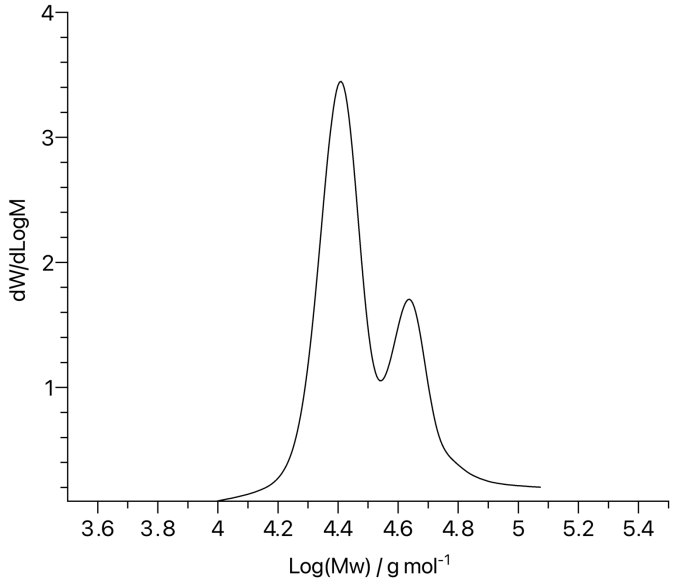

S3.1.8. GPC trace of 34% AAQ-PA-CHO

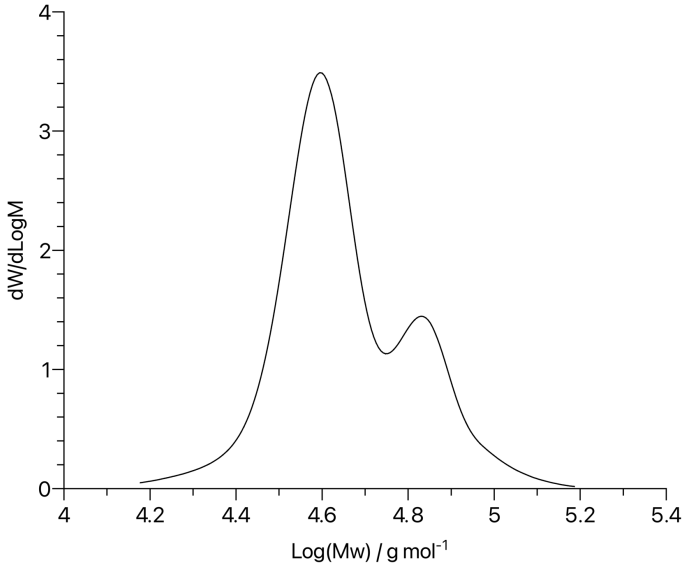

S3.1.9. GPC trace of 64% AAQ-PA-CHO

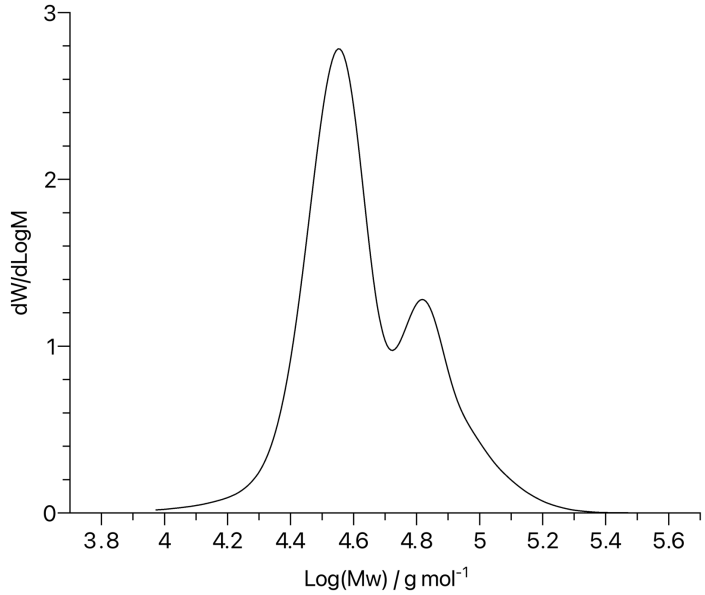

S3.1.10. GPC trace of TCPA-CHO

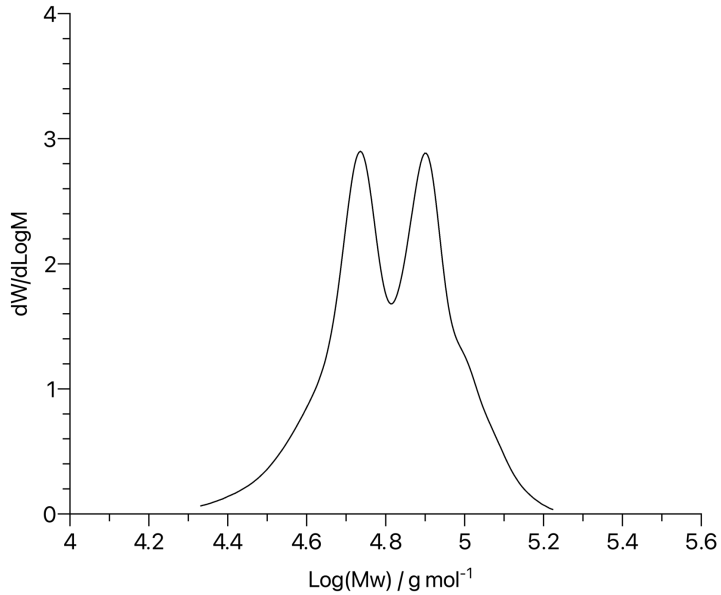

S3.1.11. GPC trace of PA-PO

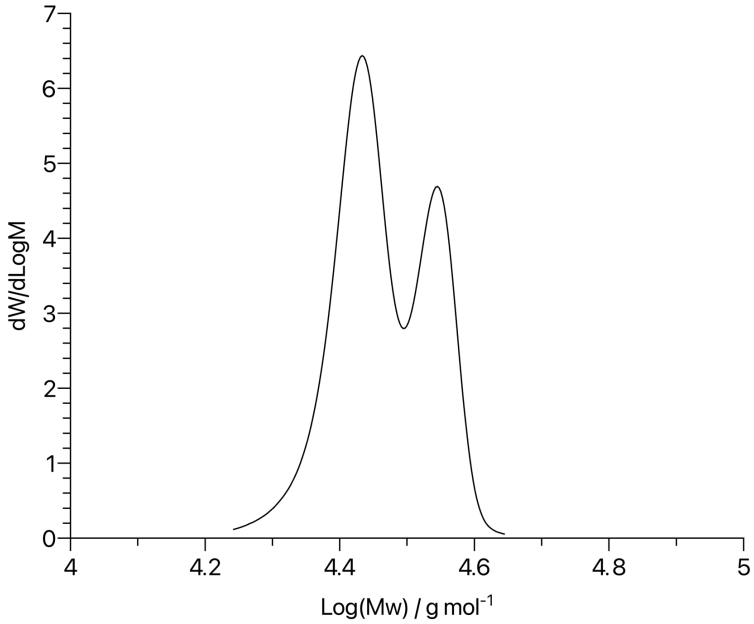

S3.1.12. GPC trace of 0.2% NAP-TCPA-CHO

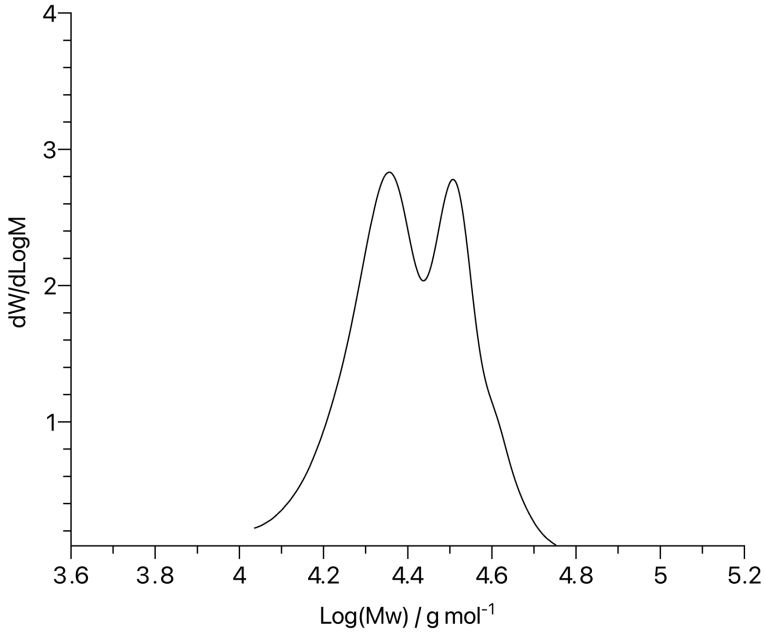

S3.1.13. GPC trace of 0.2% NAP-PA-PO

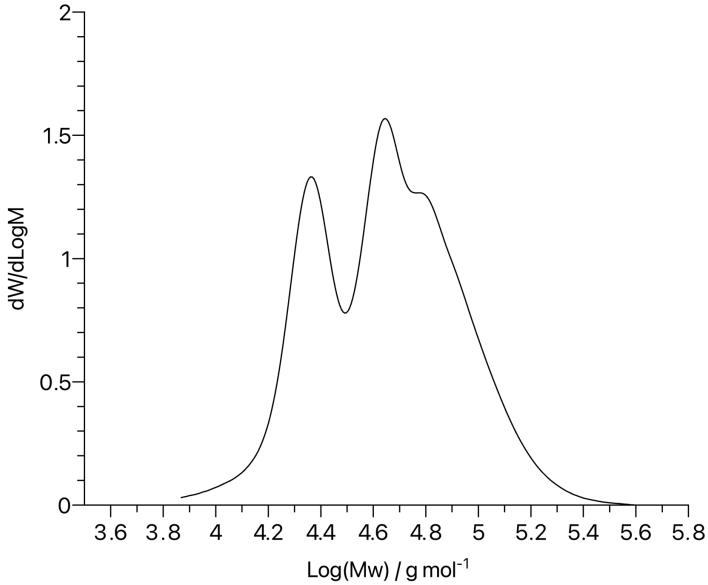

S3.1.14. GPC trace of 0.2% AAQ-TCPA-CHO

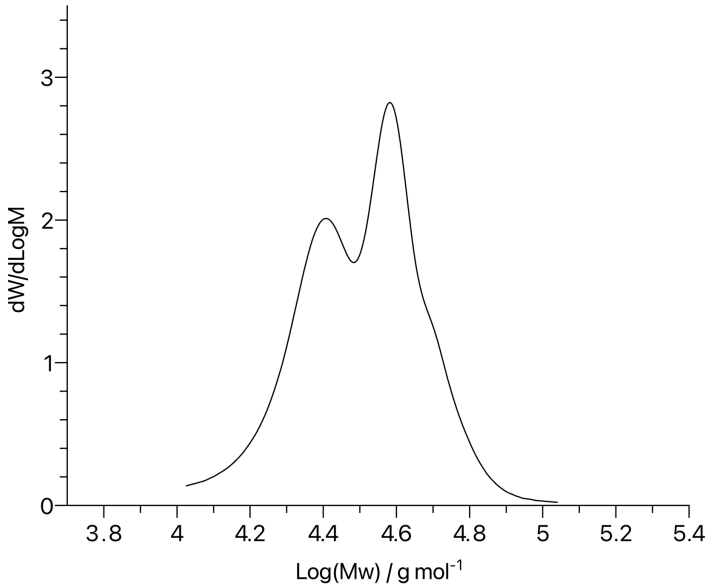

S3.1.15. GPC trace of 0.2% AAQ-PA-PO

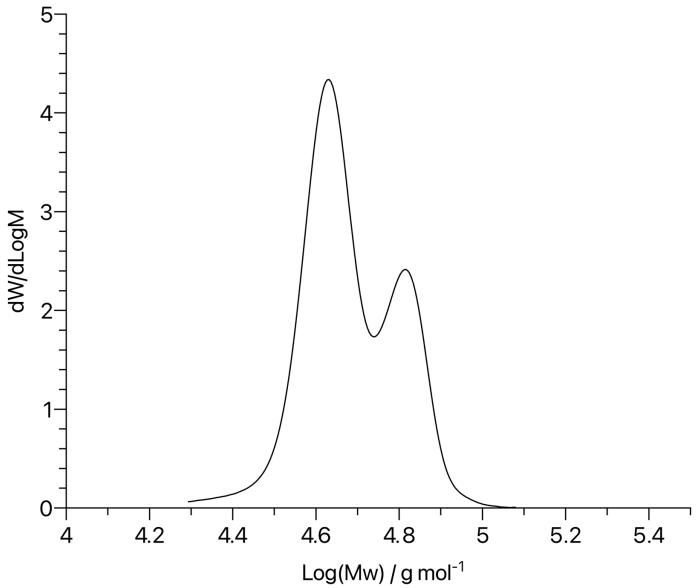

S3.1.16. GPC trace of Recycled PA-CHO

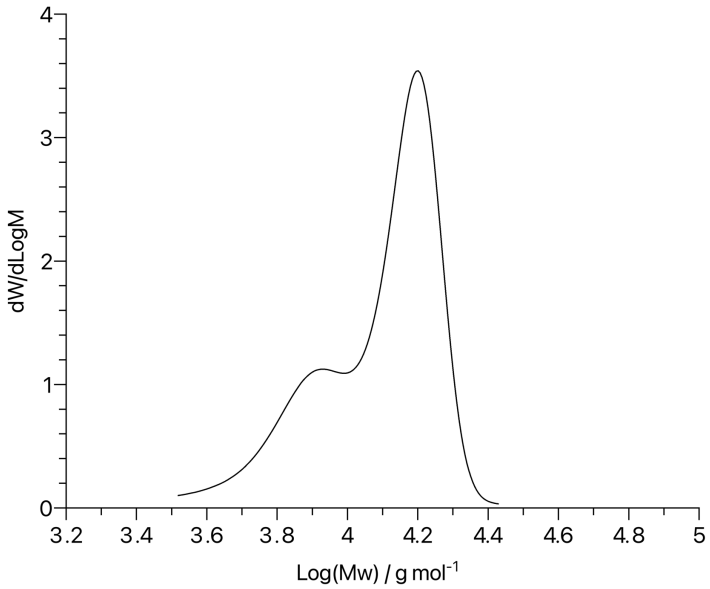

S3.2 DOSY NMR data

S3.2.1. Top to Bottom: 12%, 33%, 63% Nap-PA-CHO (Table 1: Entries 3, 4, 5 respectively). Peaks highlighted by black boxes associated with napthalimide dopant.

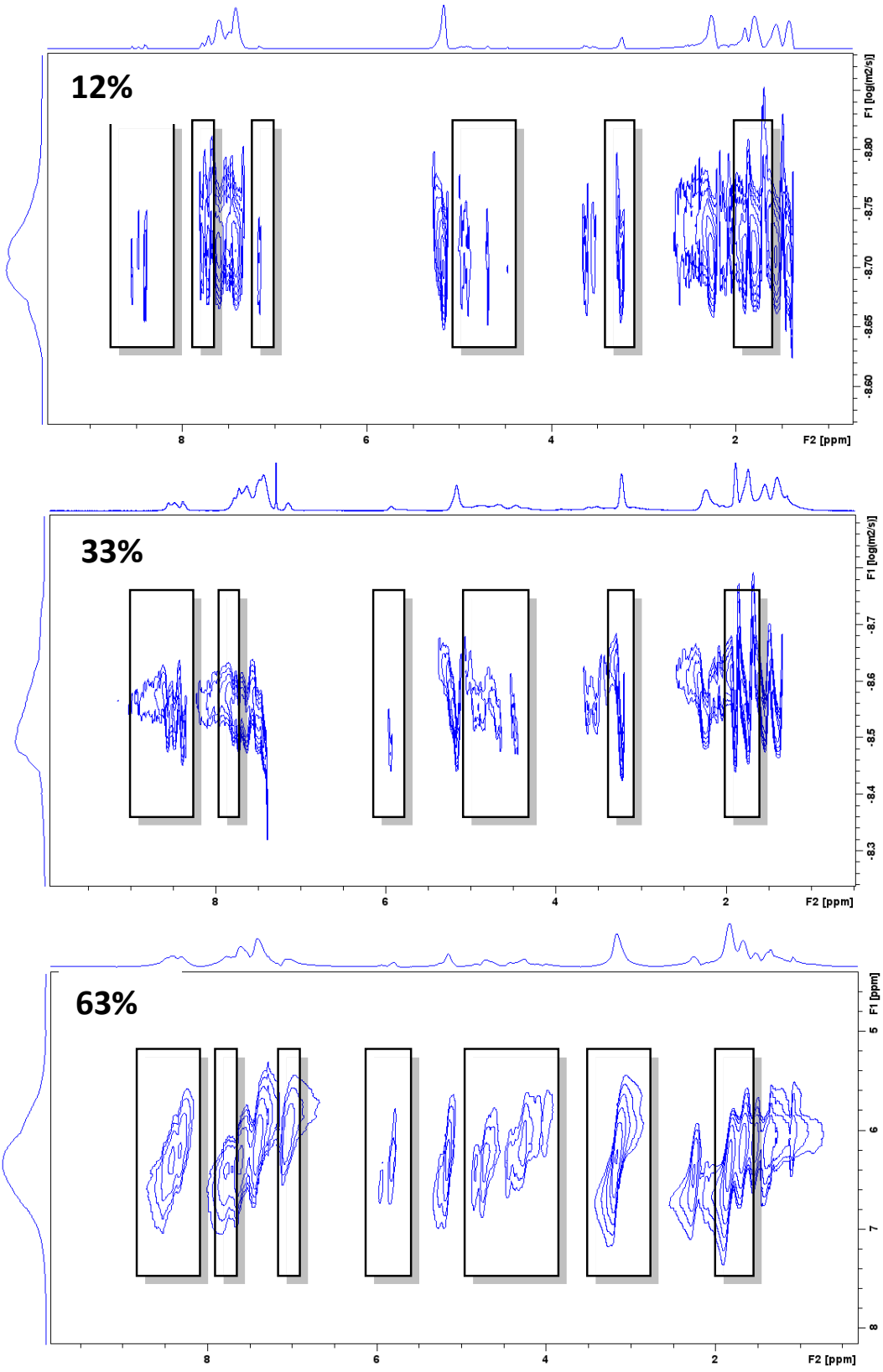

S3.2.2. Top to Bottom: 14%, 34%, 64% AAQ-PA-CHO (Table 1: Entries 7, 8, 9 respectively). Peaks highlighted by black boxes associated with aminoanthraquinone dopant. Dashed box indicates overlapping peaks with base polymer.

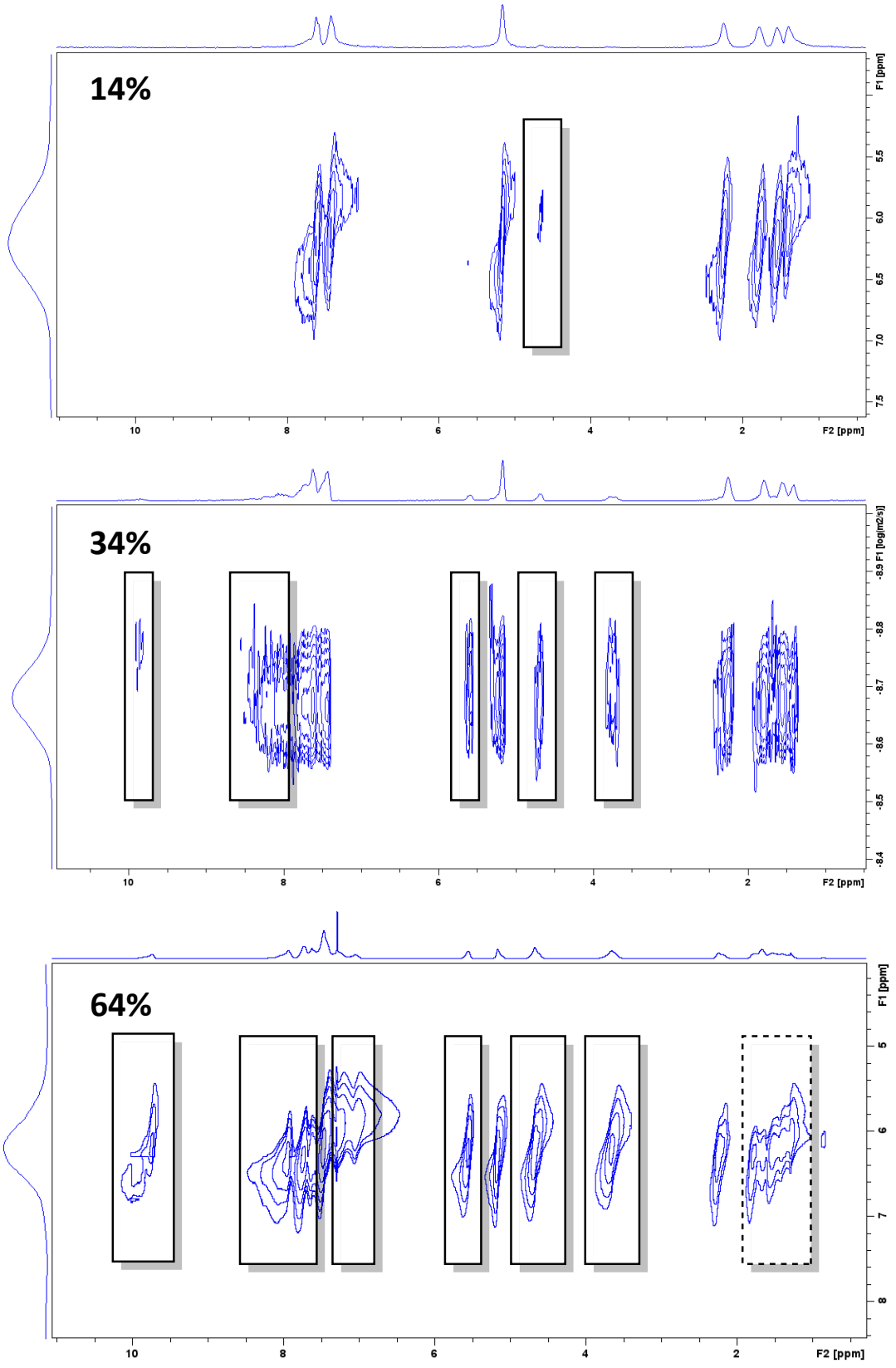

S3.3 DSC data

S3.3.1. 0.2% Nap (yellow), 0.2% AAQ (red), un-doped (black) DSC Traces (Table 1, Entries 2, 6, 1 respectively)

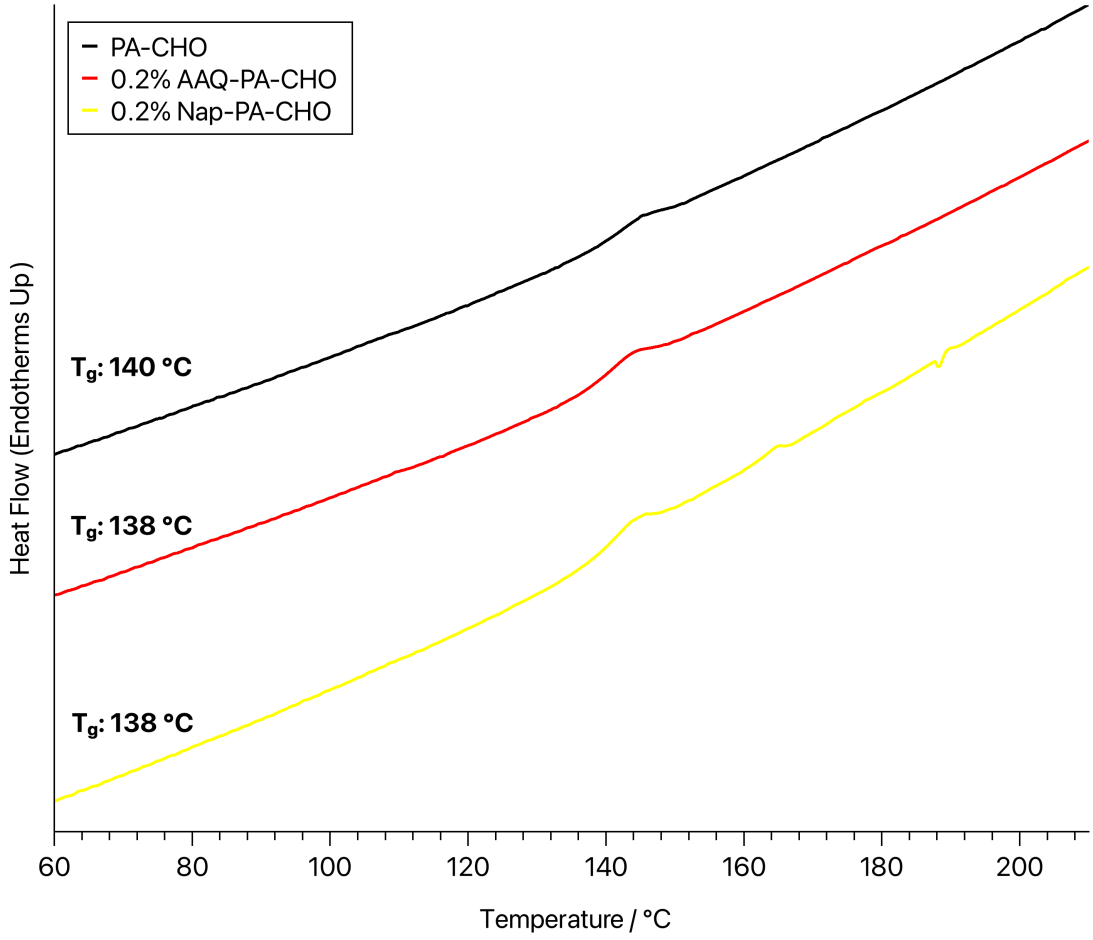

S3.3.2. 12% Nap-PA-CHO (Table 1, Entry 3)

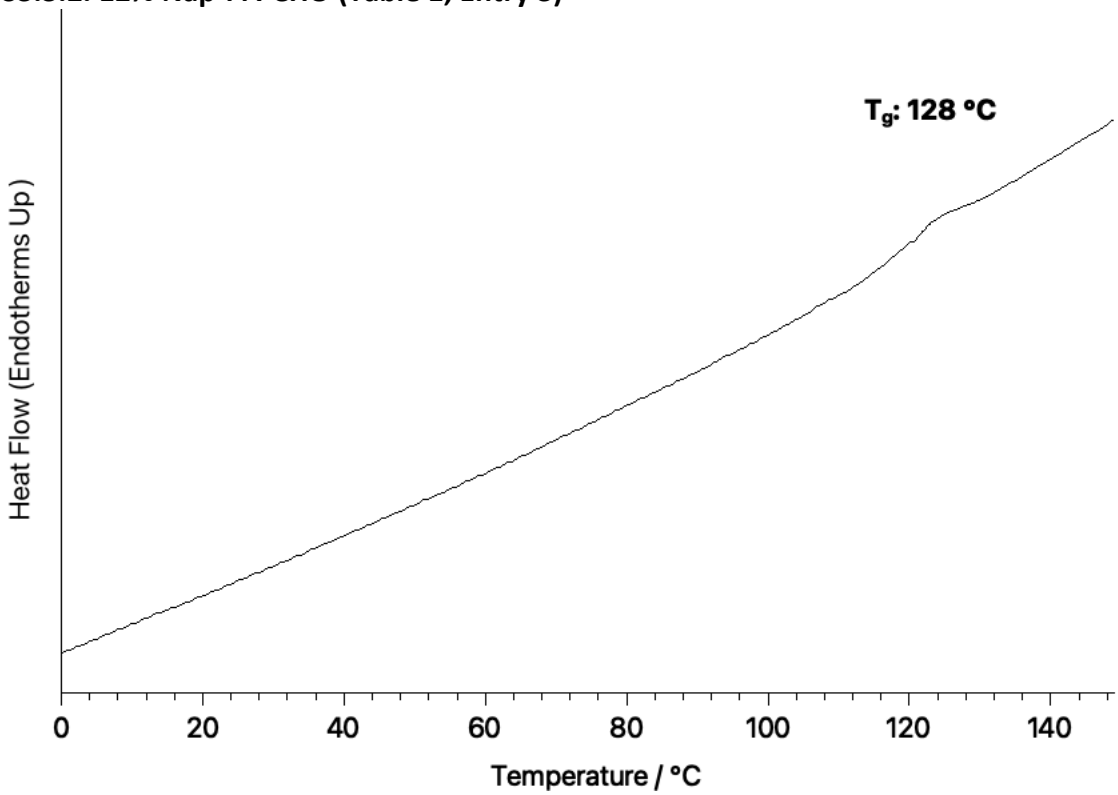

S3.3.3. 33% Nap-PA-CHO (Table 1, Entry 4)

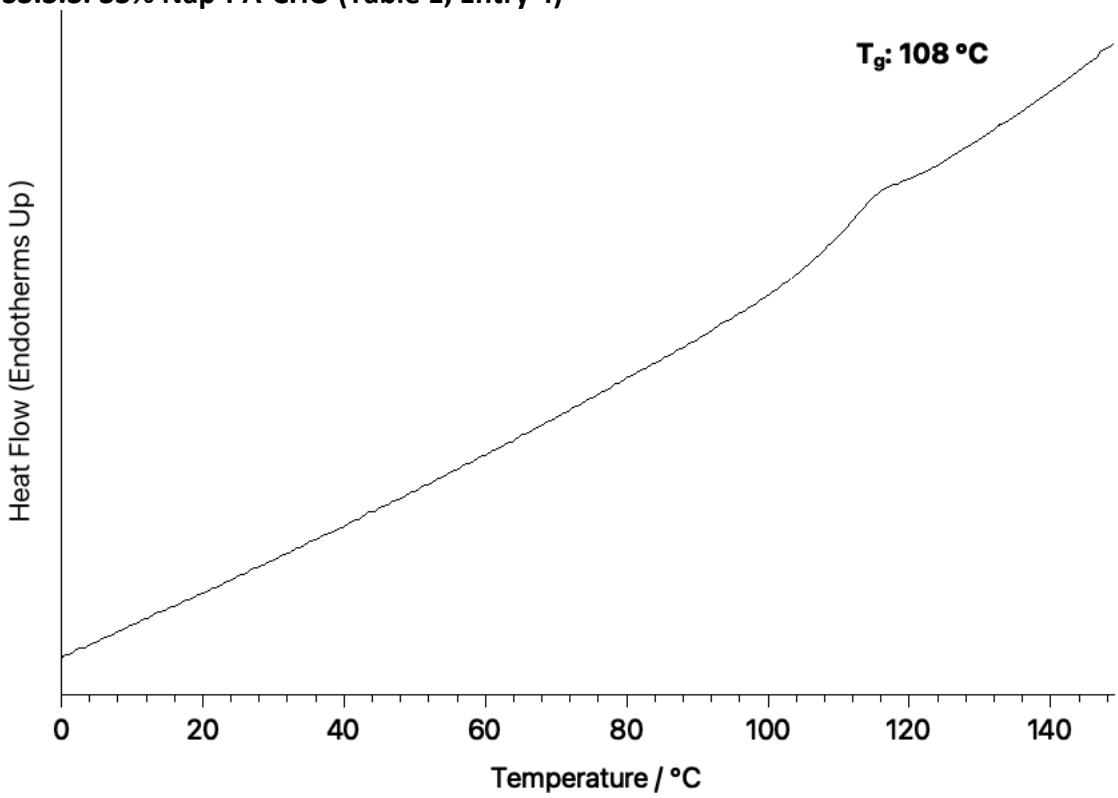

S3.3.4. 63% Nap-PA-CHO (Table 1, Entry 5)

No Transition observed

S3.3.5. 8% AAQ-PA-CHO (Table 1, Entry 7)

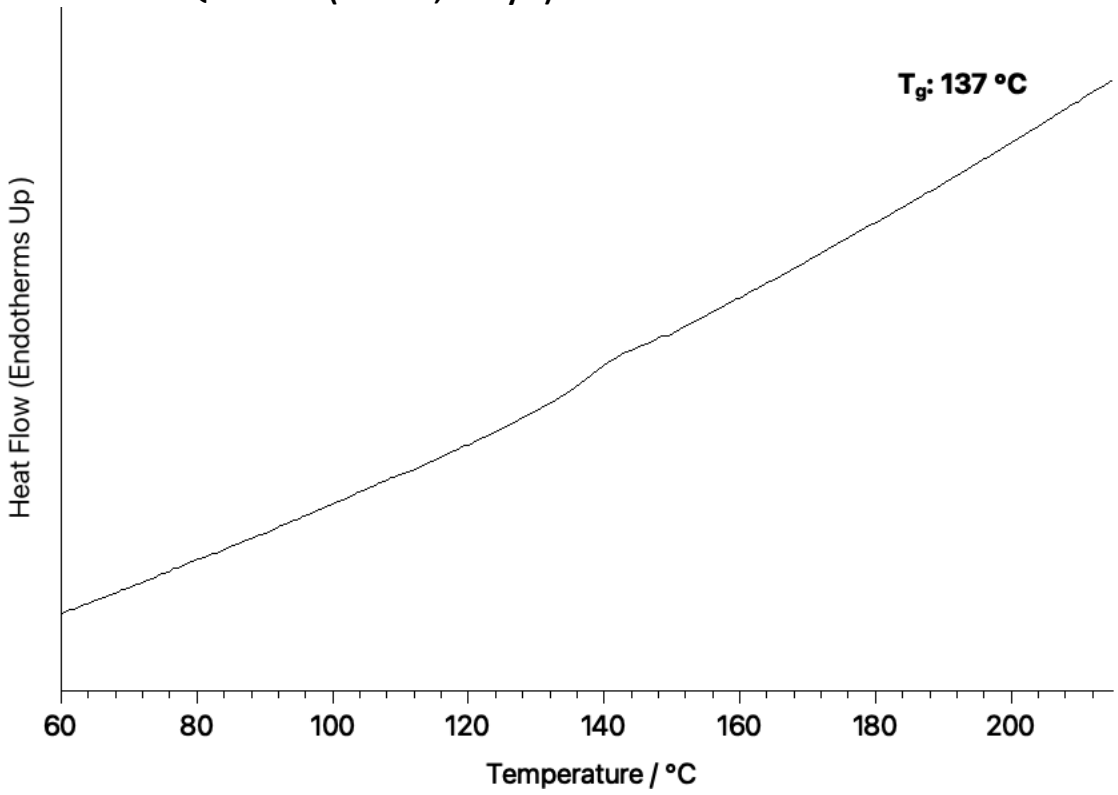

S3.3.6. 20% AAQ-PA-CHO (Table 1, Entry 8)

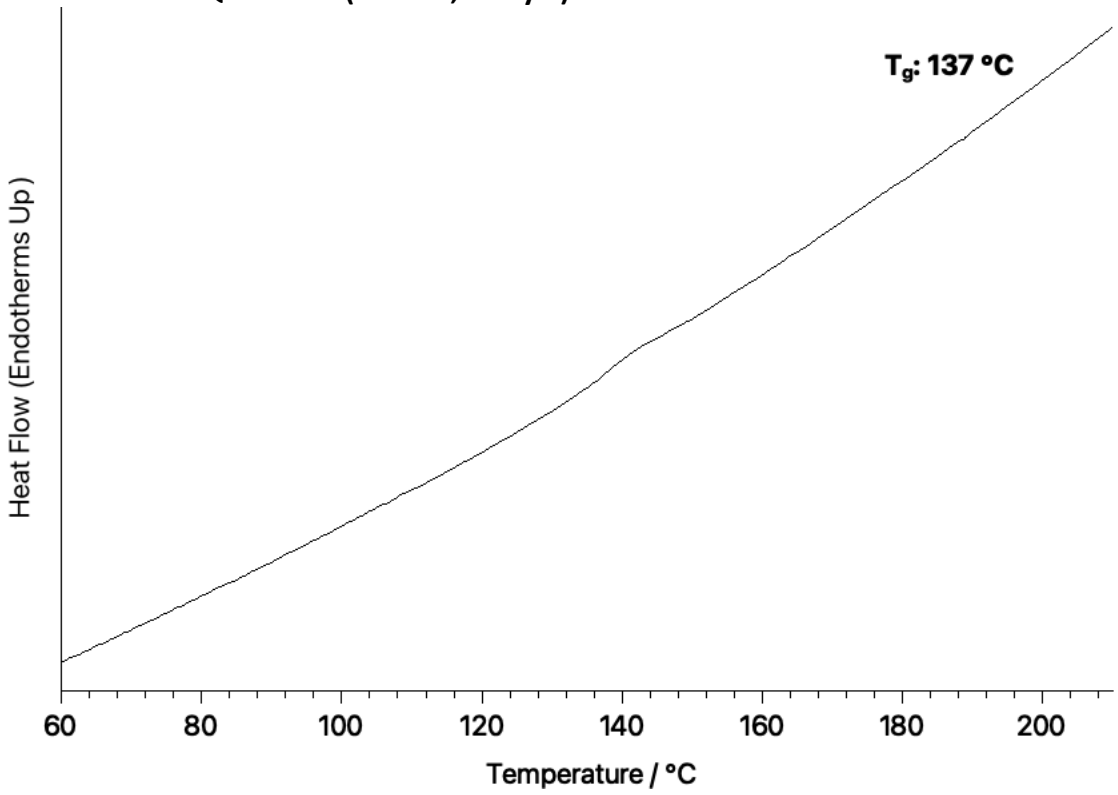

S3.3.7. 54% AAQ-PA-CHO (Table 1, Entry 9)

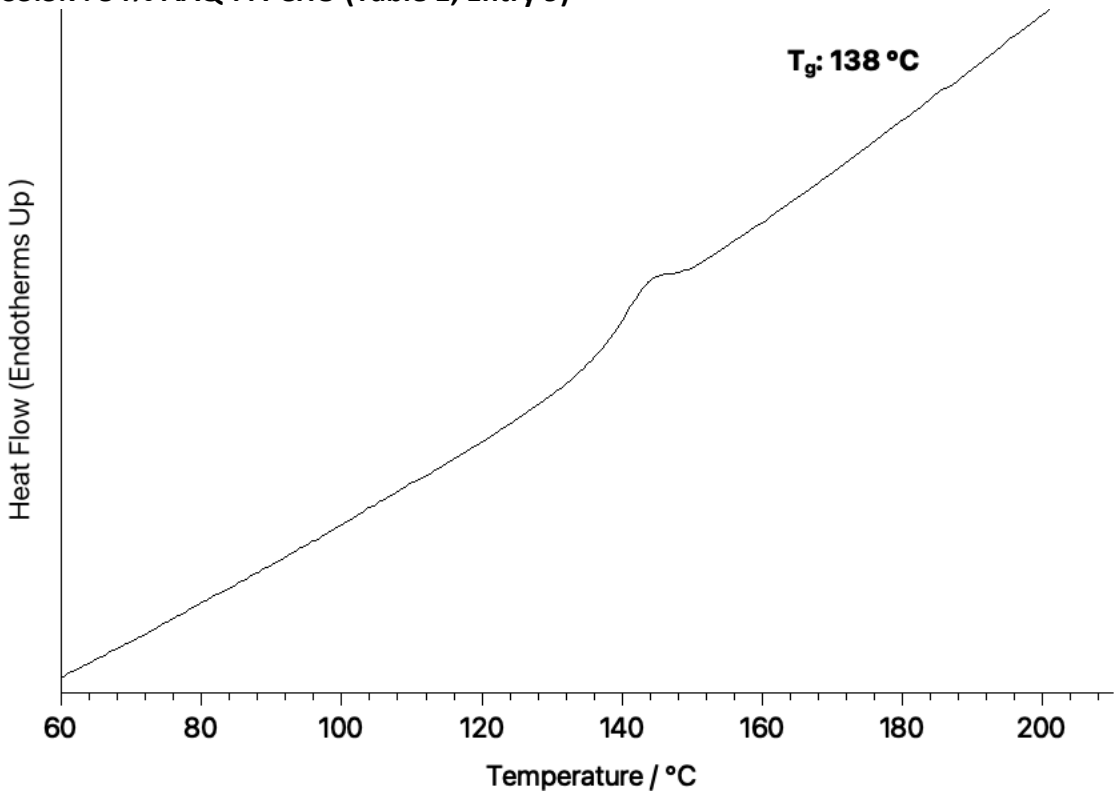

S3.3.8. TCPA-CHO (Table 1, Entry 10)

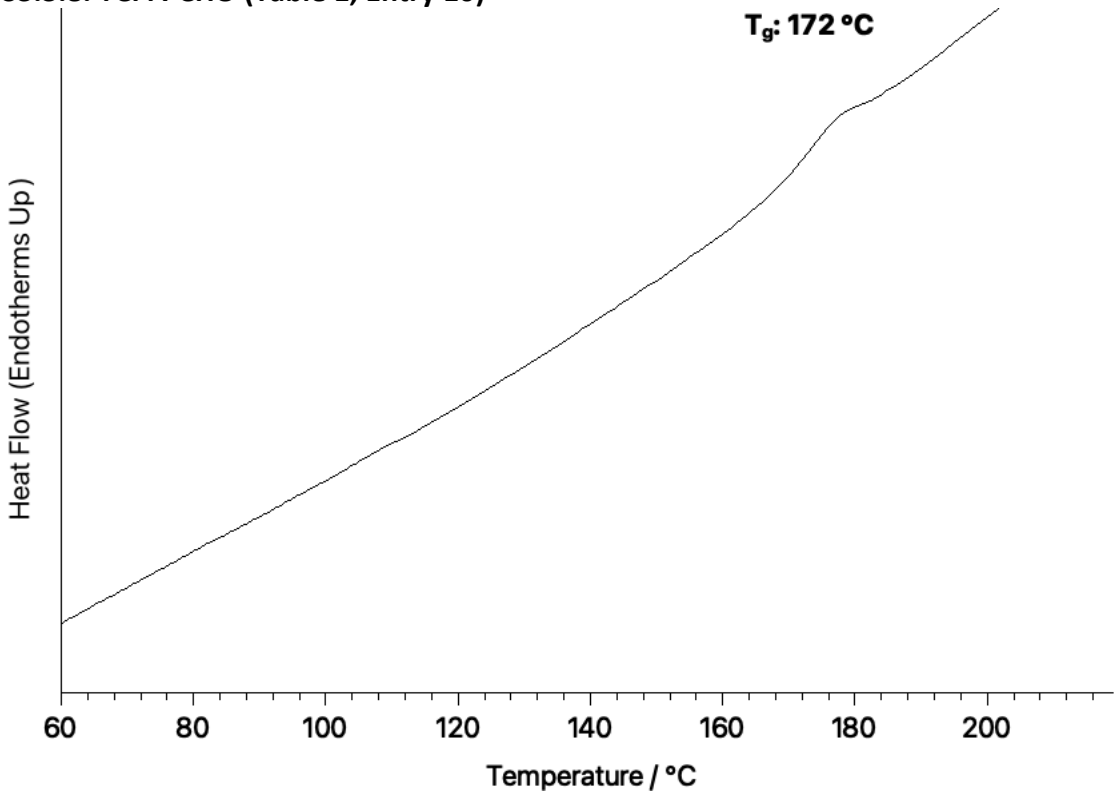

3.3.9. PA-PO (Table 1, Entry 11)

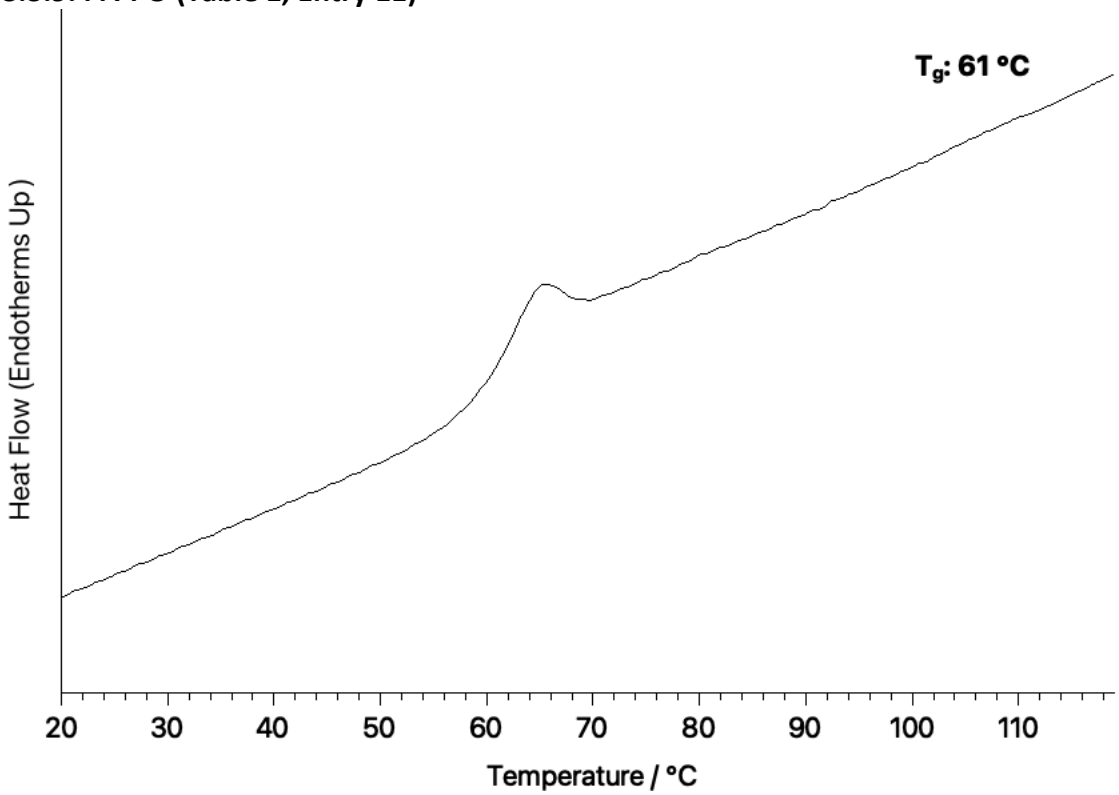

S3.3.10. Nap-TCPA-CHO (Table 1, Entry 12)

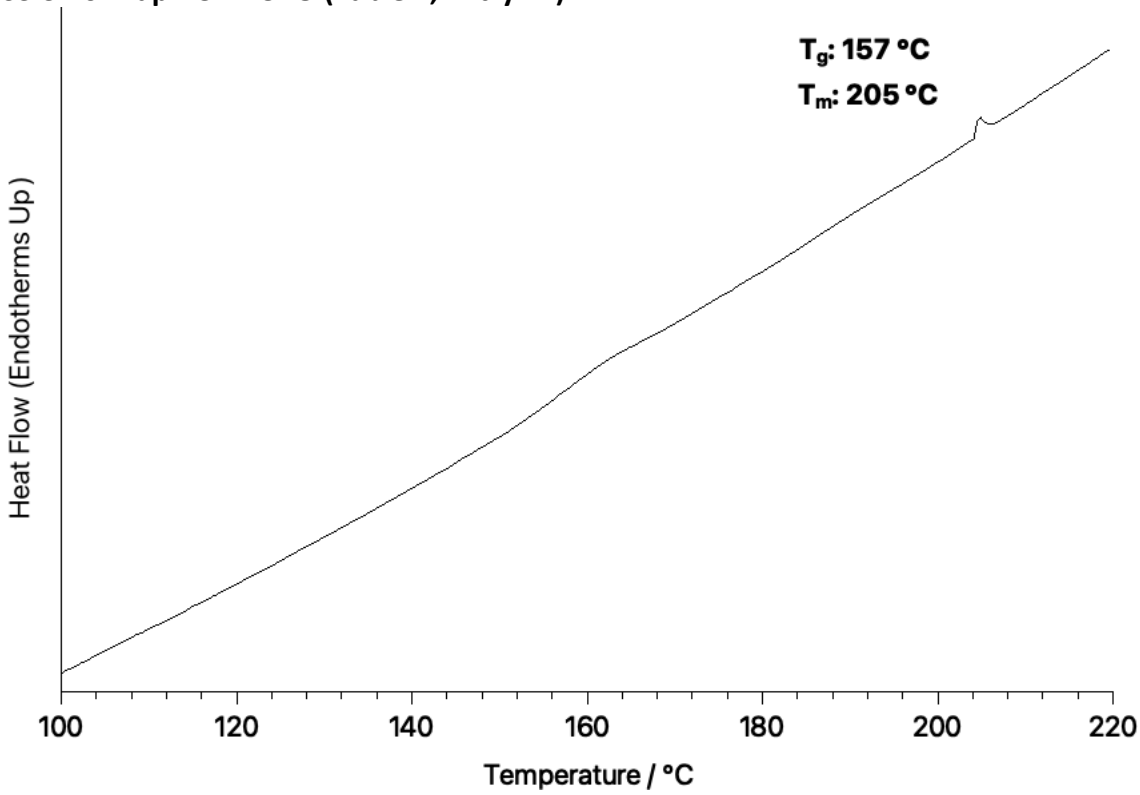

S3.3.11. Nap-PA-PO (Table 1, Entry 13)

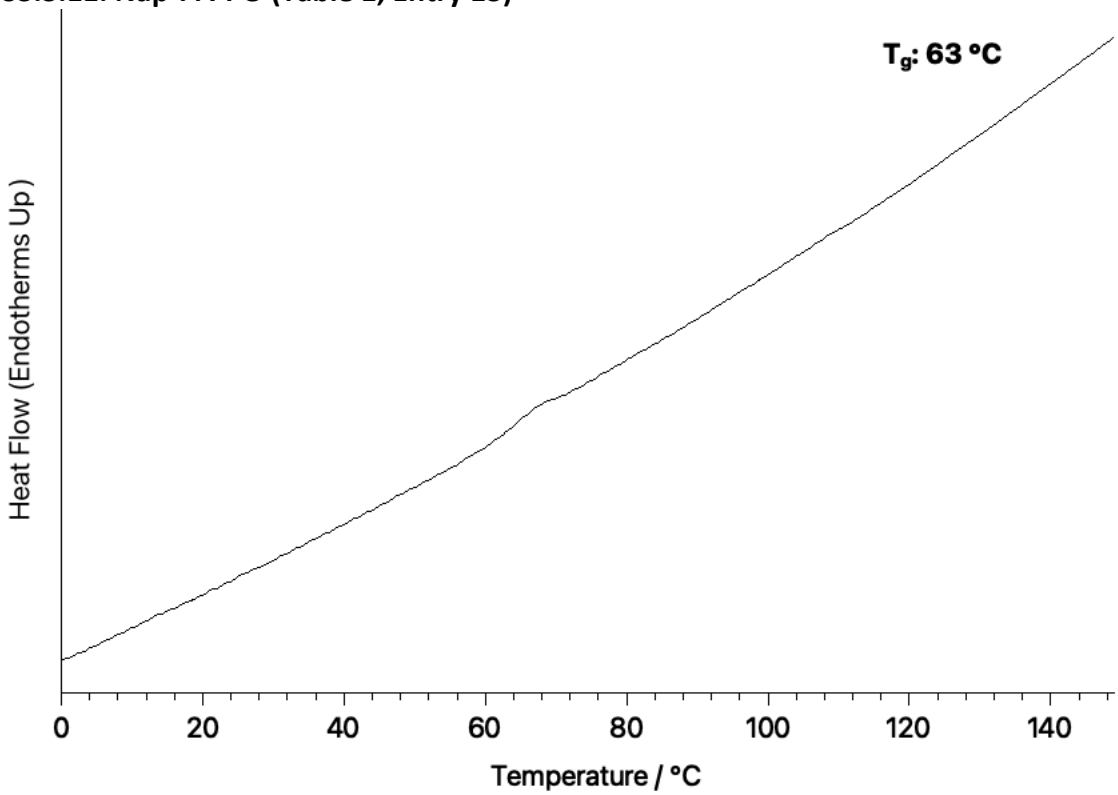

S3.3.12. AAQ-TCPA-CHO (Table 1, Entry 14)

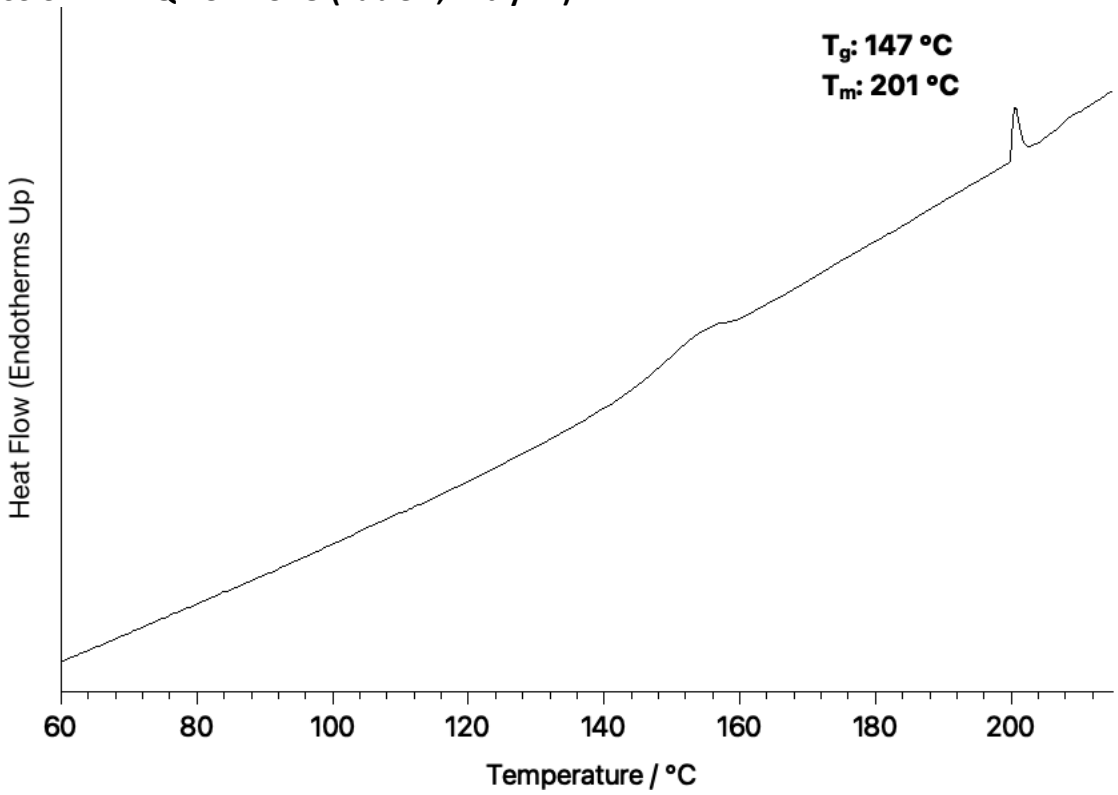

S3.3.13. AAQ-PA-PO (Table 1, Entry 15)

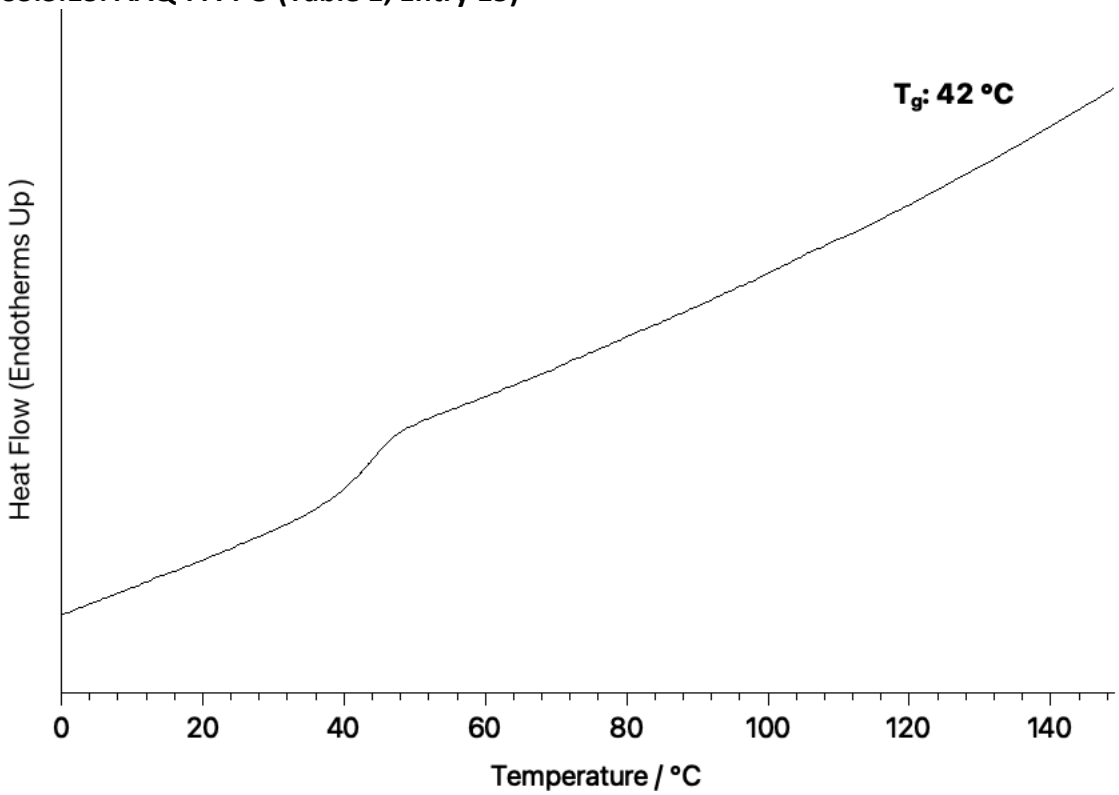

S3.3.14. Recycled PA-CHO (Table 1, Entry 16)

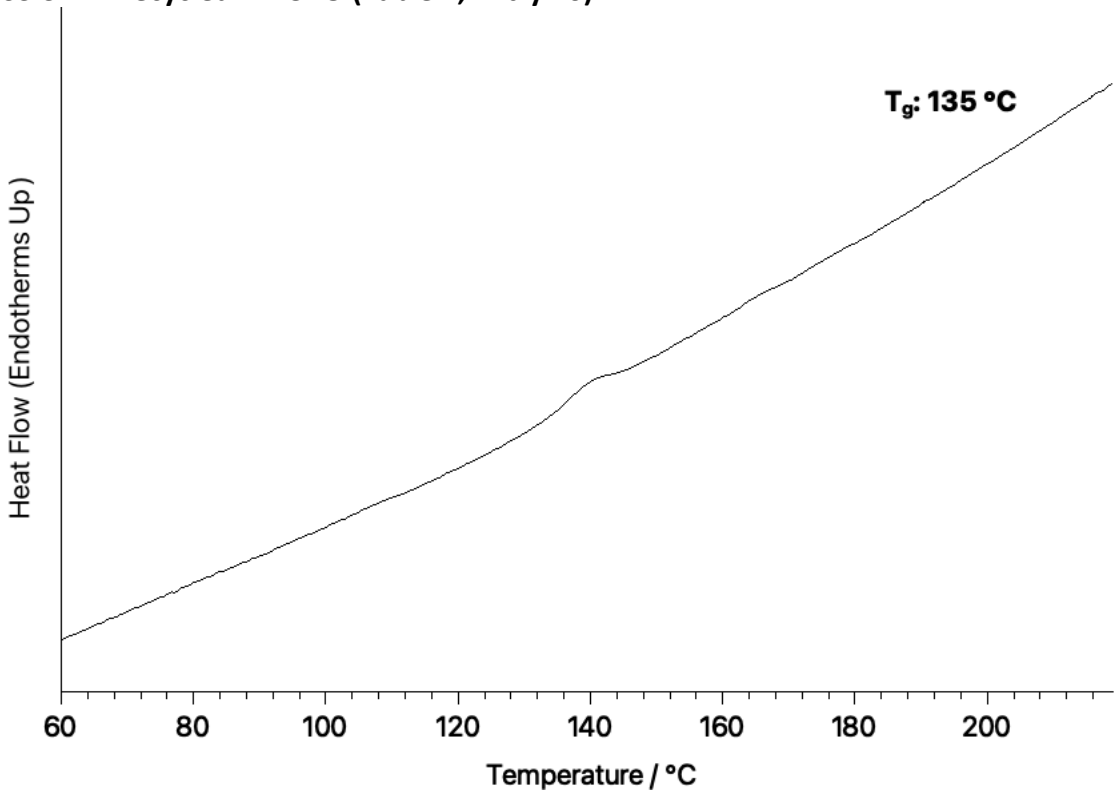

S4. Photophysical data

S4.1. UV-Vis absorption spectra of the catalyst and dopants as chloroform solutions

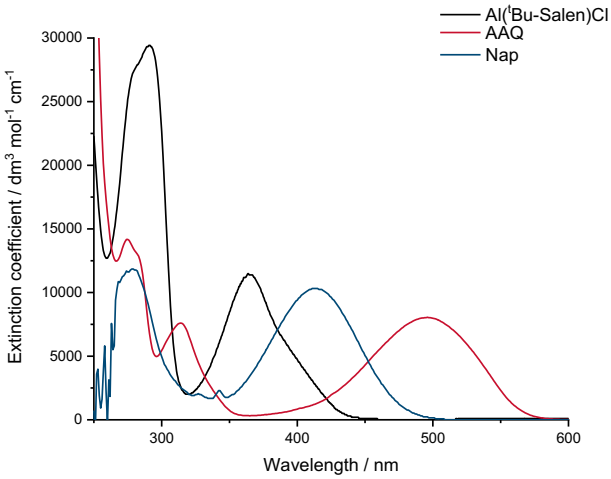

S4.2. UV-vis absorption spectra of CHO-PA, Nap-PA-CHO, and AAQ-PA-CHO as chloroform solutions

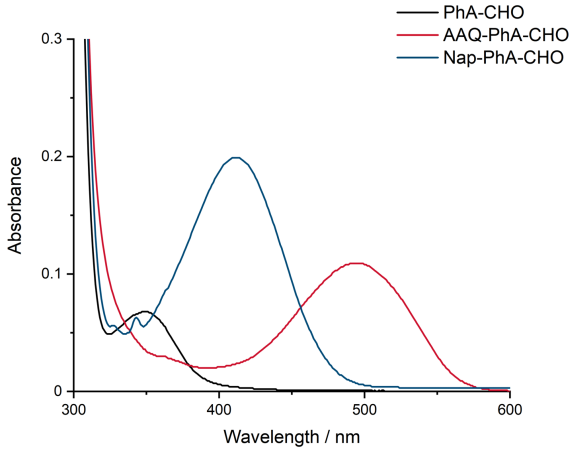

S4.3. Excitation spectra (dashed line, λ_{em} = 480 nm) and emission spectra (solid line λ_{ex} = 365 nm) of Al(tBu-Salen)Cl as a chloroform solution

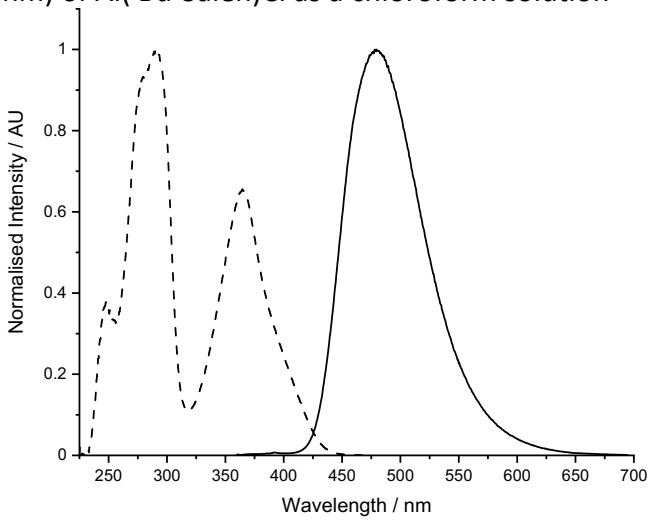

S4.4. Excitation spectra (dashed line, λ_{em} = 510 nm) and emission spectra (solid line λ_{ex} = 410 nm) of nap as a chloroform solution

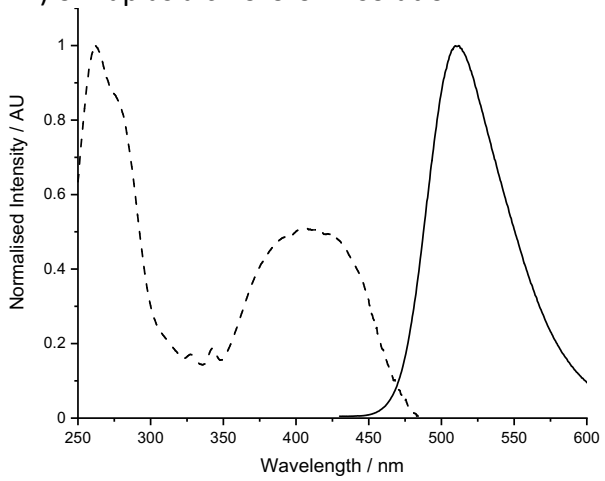

S4.5. Excitation spectra (dashed line, λ_{em} = 587 nm) and emission spectra (solid line λ_{ex} = 493 nm) of AAQ as a chloroform solution.

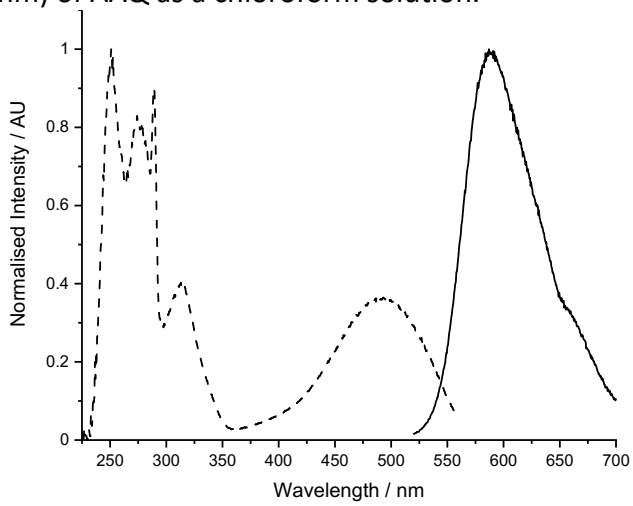

S4.6. Excitation spectra of CHO-PA (λ_{em} = 480 nm), AAQ-PA-CHO (λ_{em} = 583 nm), Nap-PhA-CHO (λ_{em} = 510 nm) as chloroform solutions

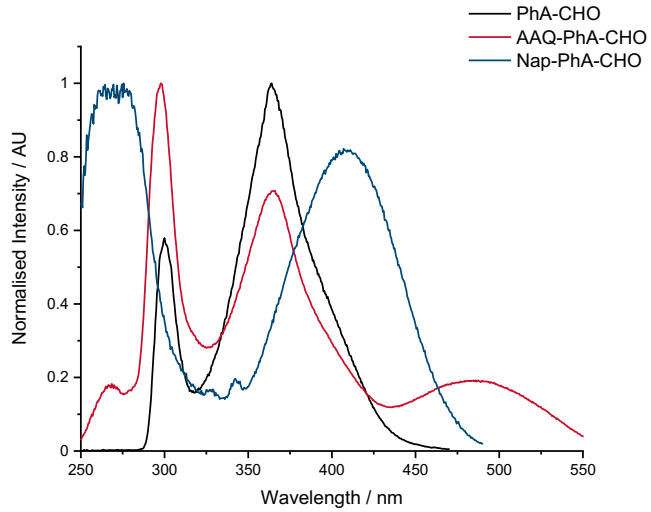

S4.7. Emission spectra of PA-CHO (λ_{ex} = 365 nm), AAQ-PA-CHO (λ_{ex} = 490 nm), Nap-PA-CHO (λ_{ex} = 410 nm) as chloroform solutions. Inset: Nap-PA-CHO under 365 nm irradiation.

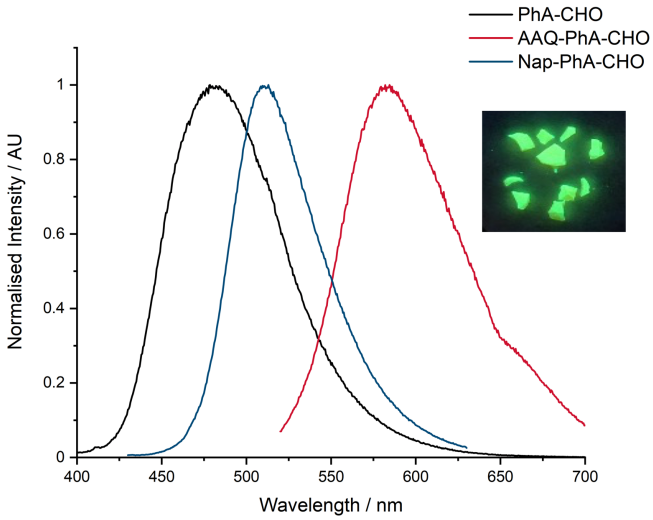

S5. Computational details

All calculations were undertaken using the Gaussian 09 program.[12] Structures were optimized without symmetry restraints using the B3LYP functional and cc-PVDZ basis set on all centers. The nature of stationary points (minimum vs. saddle point) was verified with a frequency calculation; all structures exhibited no imaginary frequencies. TD-DFT calculations were undertaken at the same level of theory as the geometry optimizations and the first 20 excited states were determined. Surfaces are drawn to an isosurface of 0.02 a.u.

S5.1. TD-DFT data

S5.1.1. Calculated HOMO (bottom), LUMO (top) molecular orbitals and geometry of Al(^{t}Bu-Salen)Cl, Nap, and AAQ (L to R) using the B3LYP functional and cc-PVDZ basis set

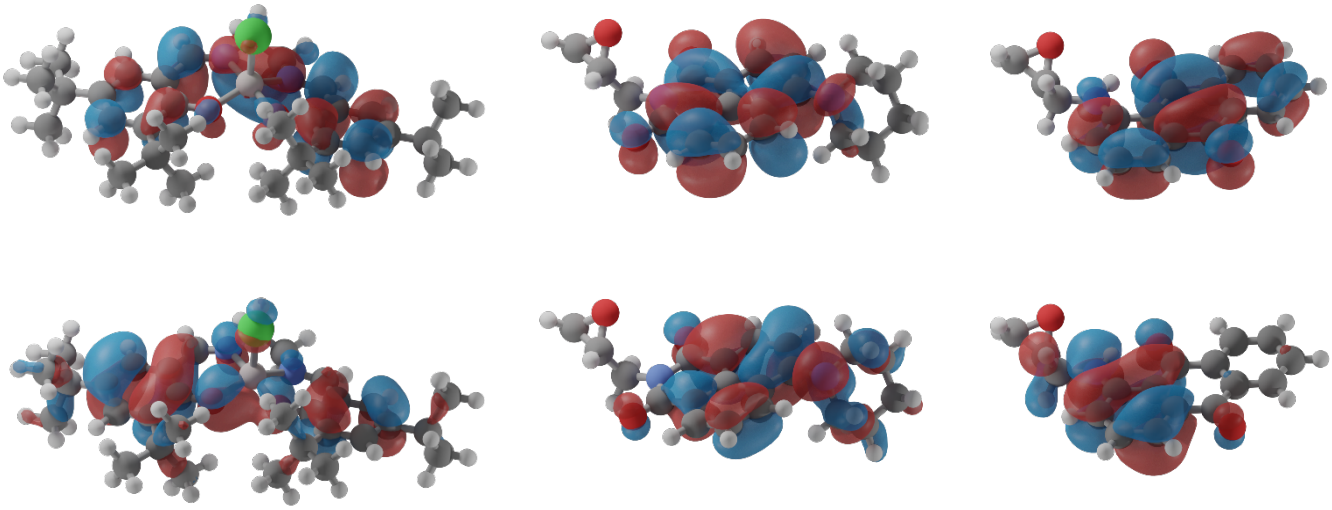

S5.1.2. 4-Piperidinyl-(N-propylene-oxide)-1,8-naphthalimide (Nap)

#	State	Transition energy (nm)	Participating MO	Transition character
1	Singlet	432.21 (0.3156)[a]	HOMO → LUMO (0.69912)[b]	Intramolecular charge transfer
2	Singlet	319.47 (0.0003)	HOMO-3 → LUMO (0.68527)	n → π*
3	Singlet	313.13 (0.0028)	HOMO-4 → LUMO (0.32246)	π → π*
	Singlet		HOMO-2 → LUMO (-0.33684)	π → π*
	Singlet		HOMO-1 → LUMO (-0.12053)	Intramolecular charge transfer
	Singlet		HOMO → LUMO (0.50654)	Intramolecular charge transfer
4	Singlet	304.55 (0.0071)	HOMO-6 → LUMO (0.12449)	n → π*
	Singlet		HOMO-4 → LUMO (0.12673)	π → π*
	Singlet		HOMO-2 → LUMO (0.21369)	π → π*
	Singlet		HOMO-1 → LUMO (0.58162)	Intramolecular charge transfer
	Singlet		HOMO → LUMO +1 (0.20705)	Intramolecular charge transfer
	Singlet		HOMO → LUMO+2 (-0.16230)	Intramolecular charge transfer
5	Singlet	291.59 (0.0539)	HOMO-4 → LUMO (0.20646)	π → π*

	Singlet		HOMO-2 → LUMO (0.51772)	π → π*
	Singlet		HOMO-1 → LUMO (-0.34793)	Intramolecular charge transfer
	Singlet		HOMO → LUMO+1 (0.13834)	Intramolecular charge transfer
	Singlet		HOMO → LUMO+2 (-0.13329)	Intramolecular charge transfer
6	Singlet	286.02 (0.1422)	HOMO-6 → LUMO (0.15480)	n → π*
	Singlet		HOMO-5 → LUMO (0.38543)	n → π*
	Singlet		HOMO → LUMO+2 (0.54450)	Intramolecular charge transfer
7	Singlet	281.65 (0.1275)	HOMO-6 → LUMO (0.22614)	n → π*
	Singlet		HOMO-5 → LUMO (0.35288)	n → π*
	Singlet		HOMO-4 → LUMO (0.23856)	π → π*
	Singlet		HOMO-3 → LUMO (-0.22639)	n → π*
	Singlet		HOMO-2 → LUMO+1 (-0.29416)	π → π*
	Singlet		HOMO → LUMO+2 (-30844)	Intramolecular charge transfer
8	Singlet	272.61 (0.1582)	HOMO-6 → LUMO (-0.27213)	n → π*
	Singlet		HOMO-5 → LUMO (-0.17013)	n → π*
	Singlet		HOMO-4 → LUMO (0.48099)	π → π*
	Singlet		HOMO-1 → LUMO+1 (-0.15821)	Intramolecular charge transfer
	Singlet		HOMO → LUMO+1 (-0.26347)	Intramolecular charge transfer
	Singlet		HOMO → LUMO+2 (0.18183)	Intramolecular charge transfer
9	Singlet	253.01 (0.0799)	HOMO-6 → LUMO (0.53703)	n → π*
	Singlet		HOMO-5 → LUMO (-0.38486)	n → π*
	Singlet		HOMO-1 → LUMO+1 (-0.15474)	Intramolecular charge transfer
	Singlet		HOMO → LUMO+2 (0.10674)	Intramolecular charge transfer
10	Singlet	235.32 (0.0160)	HOMO → LUMO+3 (0.68101)	Intramolecular charge transfer
11	Singlet	230.65 (0.0051)	HOMO-7 → LUMO (0.62820)	π → π*
	Singlet		HOMO-1 → LUMO+2 (-0.25505)	Intramolecular charge transfer
12	Singlet	226.63 (0.0018)	HOMO-8 → LUMO (0.13691)	n → π*
	Singlet		HOMO-6 → LUMO (0.11752)	n → π*
	Singlet		HOMO-5 → LUMO (0.12982)	n → π*
	Singlet		HOMO-3 → LUMO+2 (0.63443)	n → π*
13	Singlet	223.09 (0.2520)	HOMO-4 → LUMO (0.14547)	π → π*
	Singlet		HOMO-4 → LUMO+2 (-0.15267)	π → π*
	Singlet		HOMO-2 → LUMO+2 (0.25145)	π → π*
	Singlet		HOMO-1 → LUMO+1 (0.51580)	Intramolecular charge transfer

	Singlet		HOMO-1 → LUMO+2 (-0.22968)	Intramolecular charge transfer
14	Singlet	218.95 (0.0134)	HOMO-4 → LUMO+1 (0.10025)	π → π*
	Singlet		HOMO-3 → LUMO+1 (0.65837)	n → π*
	Singlet		HOMO-1 → LUMO+2 (0.18283)	Intramolecular charge transfer
15	Singlet	217.70 (0.0705)	HOMO-8 → LUMO (-0.16924)	n → π*
	Singlet		HOMO-7 → LUMO (19395)	π → π*
	Singlet		HOMO-5 → LUMO+2 (0.11387)	n → π*
	Singlet		HOMO-3 → LUMO+1 (-0.17609)	n → π*
	Singlet		HOMO-2 → LUMO+1 (-0.12791)	π → π*
	Singlet		HOMO-2 → LUMO+2 (0.22913)	π → π*
	Singlet		HOMO → LUMO+2 (0.51502)	Intramolecular charge transfer
16	Singlet	216.02 (0.0205)	HOMO-8 → LUMO (0.62407)	n → π*
	Singlet		HOMO-3 → LUMO+1 (-0.14435)	n → π*
	Singlet		HOMO-3 → LUMO+2 (-0.14895)	n → π*
	Singlet		HOMO-2 → LUMO+1 (0.16732)	π → π*
	Singlet		HOMO-1 → LUMO+2 (0.12898)	Intramolecular charge transfer
17	Singlet	215.88 (0.1109)	HOMO-8 → LUMO (-0.21120)	n → π*
	Singlet		HOMO-6 → LUMO+1 (0.10813)	n → π*
	Singlet		HOMO-4 → LUMO+1 (0.18356)	π → π*
	Singlet		HOMO–2 → LUMO+1 (0.59529)	π → π*
	Singlet		HOMO-2 → LUMO+2 (-0.11828)	π → π*
	Singlet		HOMO-1 → LUMO+1 (0.10946)	Intramolecular charge transfer
18	Singlet	214.44 (0.0725)	HOMO-7 → LUMO (-0.12850)	π → π*
	Singlet		HOMO-5 → LUMO+2 (0.10319)	n → π*
	Singlet		HOMO–4 → LUMO+1 (-0.11414)	π → π*
	Singlet		HOMO-2 → LUMO+1 (0.19519)	π → π*
	Singlet		HOMO-2 → LUMO+2 (0.53343)	π → π*
	Singlet		HOMO-1 → LUMO+1 (-0.26311)	Intramolecular charge transfer
19	Singlet	211.47 (0.0122)	HOMO-7 → LUMO+1 (-0.14348)	π → π*
	Singlet		HOMO-6 → LUMO+2 (0.12115)	n → π*
	Singlet		HOMO-5 → LUMO+2 (0.11779)	n → π*
	Singlet		HOMO-4 → LUMO+2 (0.60830)	π → π*
	Singlet		HOMO-3 → LUMO+2 (-0.12052)	n → π*
	Singlet		HOMO-1 → LUMO+1 (0.15944)	Intramolecular charge transfer
20	Singlet	207.94 (0.0202)	HOMO-13 → LUMO (-0.11291)	σ → π*
	Singlet		HOMO-12 → LUMO (0.23101)	σ → π*
	Singlet		HOMO-9 → LUMO (0.62460)	σ → π*

[a] Oscillator strength, [b] Orbital coefficient

S5.1.3. [Al(^{t}Bu-Salen)Cl] (1)

#	State	Transition energy (nm)	Participating MO	Transition character
1	Singlet	399.29 (0.0180)[a]	HOMO → LUMO (0.70088)[b]	π → π*
2	Singlet	370.92 (0.0825)	HOMO-1 → LUMO (0.69989)	π → π*
3	Singlet	352.33 (0.0716)	HOMO → LUMO+1 (0.69735)	π → π*
4	Singlet	338.40 (0.0183)	HOMO-1 → LUMO+1 (069507)	π → π*
5	Singlet	296.28 (0.2664)	HOMO-4 → LUMO (0.31937)	n → π*
	Singlet		HOMO-2 → LUMO (0.60282)	π → π*
6	Singlet	289.60 (0.0869)	HOMO-5 → LUMO (0.10936)	n → π*
	Singlet		HOMO-5 → LUMO+1 (-0.11742)	n → π*
	Singlet		HOMO-4 → LUMO (0.52743)	n → π*
	Singlet		HOMO-3 → LUMO (-0.20988)	π → π*
	Singlet		HOMO-2 → LUMO (-0.34953)	π → π*
7	Singlet	282.00 (0.1368)	HOMO-4 → LUMO (0.19365)	n → π*
	Singlet		HOMO-3 → LUMO (0.63112)	π → π*
	Singlet		HOMO-2 → LUMO+1 (-0.19532)	π → π*
8	Singlet	248.06 (0.0086)	HOMO-7 → LUMO (0.16720)	n → π*
	Singlet		HOMO-6 → LUMO (-0.14946)	n → π*
	Singlet		HOMO-5 → LUMO (-0.38869)	n → π*
	Singlet		HOMO-5 → LUMO+1 (-0.11841)	n → π*
	Singlet		HOMO-4 → LUMO (0.15448)	n → π*
	Singlet		HOMO-4 → LUMO+1 (0.46111)	n → π*
	Singlet		HOMO-2 → LUMO+1 (0.12895)	π → π*
9	Singlet	266.05 (0.1982)	HOMO-4 → LUMO (0.12898)	n → π*
	Singlet		HOMO-3 → LUMO (0.14504)	π → π*
	Singlet		HOMO-3 → LUMO+1 (0.11792)	π → π*
	Singlet		HOMO-2 → LUMO+1 (0.63455)	π → π*
10	Singlet	264.37 (0.1570)	HOMO-3 → LUMO+1 (0.67728)	π → π*
	Singlet		HOMO-2 → LUMO+1 (-0.10462)	π → π*
11	Singlet	257.68 (0.0057)	HOMO-6 → LUMO (-0.44044)	n → π*
	Singlet		HOMO-5 → LUMO (0.47594)	n → π*
	Singlet		HOMO-4 → LUMO+1 (0.23623)	n → π*
12	Singlet	253.28 (0.0090)	HOMO-6 → LUMO (0.24968)	n → π*
	Singlet		HOMO-6 → LUMO (0.50485)	n → π*
	Singlet		HOMO-5 → LUMO (0.25638)	n → π*
	Singlet		HOMO-4 → LUMO+1 (0.30305)	n → π*
13	Singlet	246.82 (0.0106)	HOMO-7 → LUMO (0.62813)	n → π*
	Singlet		HOMO-6 → LUMO (-0.10701)	n → π*
	Singlet		HOMO-5 → LUMO+1 (0.10712)	n → π*
	Singlet		HOMO-4 → LUMO+1 (-0.26976)	n → π*
14	Singlet	244.02 (0.0092)	HOMO-5 → LUMO+1 (0.64107)	n → π*
	Singlet		HOMO-4 → LUMO (0.17026)	n → π*

	Singlet		HOMO-4 → LUMO+1 (0.19721)	n → π*
15	Singlet	238.62 (0.0081)	HOMO-6 → LUMO+1 (0.67225)	n → π*
	Singlet		HOMO-5 → LUMO+1 (-0.11396)	n → π*
16	Singlet	237.62 (0.3512)	HOMO → LUMO+2 (0.65699)	π → π*
17	Singlet	233.46 (0.0026)	HOMO-7 → LUMO+1 (0.67732)	n → π*
	Singlet		HOMO-6 → LUMO+1 (0.10054)	n → π*
18	Singlet	231.37 (0.0808)	HOMO-1 → LUMO+4 (0.12912)	π → π*
	Singlet		HOMO → LUMO+3 (0.65082)	π → π*
	Singlet		HOMO → LUMO+5 (0.11749)	π → π*
19	Singlet	227.27 (0.0739)	HOMO-1 → LUMO+2 (0.66162)	π → π*
	Singlet		HOMO-1 → LUMO+4 (-0.11888)	π → π*
20	Singlet	224.75 (0.0548)	HOMO-1 → LUMO+3 (0.63540)	π → π*
	Singlet		HOMO-1 → LUMO4 (-0.10150)	π → π*
	Singlet		HOMO → LUMO+2 (0.12103)	π → π*
	Singlet		HOMO → LUMO+4 (0.13202)	π → π*

[a] Oscillator strength, [b] Orbital coefficient

S5.1.4. 1-(propylene-oxide)aminoanthraquinone (AAQ)

#	State	Transition energy (nm)	Participating MO	Transition character
1	Singlet	495.98 (0.1536)[a]	HOMO → LUMO (0.70376)[b]	Intramolecular charge transfer
2	Singlet	411.06 (0.0001)	HOMO-1 → LUMO (-0.11031)	n → π*
	Singlet		HOMO-4 → LUMO+1 (-0.10167)	n → π*
	Singlet		HOMO-1 → LUMO (0.68612)	n → π*
3	Singlet	374.61 (0.0000)	HOMO-6 → LUMO (0.15178)	n → π*
	Singlet		HOMO-4 → LUMO (0.65884)	n → π*
	Singlet		HOMO-1 → LUMO (0.11022)	n → π*
	Singlet		HOMO-1 → LUMO+1 (-0.14864)	n → π*
4	Singlet	340.15 (0.0014)	HOMO-2 → LUMO (0.65851)	π → π*
	Singlet		HOMO → LUMO+1 (0.24253)	Intramolecular charge transfer
5	Singlet	323.87 (0.0152)	HOMO-3 → LUMO (0.46291)	π → π*
	Singlet		HOMO-2 → LUMO (-0.19470)	π → π*
	Singlet		HOMO → LUMO+1 (0.47970)	Intramolecular charge transfer
6	Singlet	319.76 (0.1547)	HOMO-3 → LUMO (0.50866)	π → π*
	Singlet		HOMO-2 → LUMO (0.14162)	π → π*
	Singlet		HOMO → LUMO+1 (-0.45082)	Intramolecular charge transfer
7	Singlet	291.35 (0.0011)	HOMO-6 → LUMO (0.68257)	n → π*
	Singlet		HOMO-4 → LUMO (-0.16115)	n → π*
8	Singlet	279.96 (0.1671)	HOMO-5 → LUMO (0.67769)	π → π*
	Singlet		HOMO-2 → LUMO+2 (-0.10307)	π → π*
9	Singlet	257.71 (0.0060)	HOMO → LUMO+2 (0.69272)	Intramolecular charge transfer
10	Singlet	266.46 (0.0000)	HOMO-4 → LUMO (0.14740)	n → π*

	Singlet		HOMO-1 → LUMO+1 (0.68482)	n → π*
11	Singlet	250.74 (0.0002)	HOMO-6 → LUMO+1 (0.13533)	n → π*
	Singlet		HOMO-4 → LUMO+1 (066881)	n → π*
	Singlet		HOMO-1 → LUMO (0.11290)	n → π*
12	Singlet	249.68 (0.0184)	HOMO-8 → LUMO (0.11925)	n → π*
	Singlet		HOMO-7 → LUMO ((0.60408)	π → π*
	Singlet		HOMO-2 → LUMO+1 (0.21690)	π → π*
	Singlet		HOMO → LUMO+3 (0.18802)	Intramolecular charge transfer
13	Singlet	241.19 (0.5560)	HOMO-7 → LUMO (-0.10415)	π → π*
	Singlet		HOMO-3 → LUMO+2 (-0.16825)	π → π*
	Singlet		HOMO-2 → LUMO+1 (0.57612)	π → π*
	Singlet		HOMO → LUMO+3 (-0.32487)	Intramolecular charge transfer
14	Singlet	234.21 (0.1684)	HOMO-8 → LUMO (0.14000)	n → π*
	Singlet		HOMO-7 → LUMO (-0.24847)	π → π*
	Singlet		HOMO-5 → LUMO+1 (0.19732)	π → π*
	Singlet		HOMO-3 → LUMO+2 (-0.17839)	π → π*
	Singlet		HOMO-2 → LUMO+1 (0.18444)	π → π*
	Singlet		HOMO → LUMO+3 (0.53606)	Intramolecular charge transfer
15	Singlet	231.58 (0.0114)	HOMO-3 → LUMO (0.67992)	π → π*
	Singlet		HOMO-2 → LUMO+1 (0.10857)	π → π*
16	Singlet	229.42 (0.0035)	HOMO-8 → LUMO (0.63135)	n → π*
	Singlet		HOMO-7 → LUMO (-0.12032)	π → π*
	Singlet		HOMO-5 → LUMO+1 (-0.22624)	π → π*
	Singlet		HOMO-3 → LUMO+2 (0.10150)	π → π*
17	Singlet	226.81 (0.0011)	HOMO-1 → LUMO+2 (0.69981)	n → π*
18	Singlet	224.32 (0.1103)	HOMO-8 → LUMO (0.22779)	n → π*
	Singlet		HOMO-7 → LUMO (0.15116)	π → π*
	Singlet		HOMO-5 → LUMO+1 (0.55229)	π → π*
	Singlet		HOMO-3 → LUMO+2 (-0.15760)	π → π*
	Singlet		HOMO-2 → LUMO+1 (-0.18294)	π → π*
	Singlet		HOMO → LUMO+3 (-0.18025)	Intramolecular charge transfer
19	Singlet	219.70 (0.005)	HOMO-6 → LUMO+1 (0.68694)	n → π*
	Singlet		HOMO-4 → LUMO+1 (-0.14405)	n → π*
20	Singlet	214.13 (0.0001)	HOMO-9 → LUMO (0.21631)	σ → π*
	Singlet		HOMO-6 → LUMO+2 (0.12804)	n → π*
	Singlet		HOMO-4 → LUMO+2 (0.65221)	n → π*

[a] Oscillator strength, [b] Orbital coefficient

S5.2. Cartesian coordinates of calculated species

S5.2.1. [Al(Salen)Cl] (1)

C 0.68086400 -3.93467000 0.19857600
H 1.35703500 -4.72835700 -0.15520400

H 0.36442800 -4.16995200 1.22858800
C -0.54895600 -3.80208400 -0.70312300
H -1.24858600 -4.64011500 -0.55933500
H -0.22911500 -3.79441300 -1.75975200
N 1.32190200 -2.62245900 0.19621400
N -1.18311000 -2.51225900 -0.39278600
C 2.60530400 -2.51178900 0.04968600
H 3.20506200 -3.43204200 -0.02558100
C -2.46513200 -2.38237600 -0.58271900
H -3.02429000 -3.26277700 -0.93472800
C 3.32505100 -1.27179900 -0.03852100
C 2.64853100 -0.01533200 -0.09834000
C 4.73775200 -1.34991300 -0.11920500
C 3.44017200 1.17026000 -0.25819900
C 5.51824900 -0.21530200 -0.24813100
H 5.18821700 -2.34241600 -0.07281100
C 4.82540800 1.01951500 -0.31609900
H 5.42591900 1.92074100 -0.42510400
C -3.23483900 -1.19142000 -0.37900600
C -4.63467600 -1.28872400 -0.56243700
C -2.61880700 0.05505300 -0.03321000
C -5.46774000 -0.19334300 -0.40299800
H -5.04256300 -2.26617700 -0.83225000
C -3.46468100 1.19950500 0.13159200
C -4.83872600 1.02593800 -0.05517700
H -5.47369300 1.89707200 0.07849700
O -1.31088700 0.14832000 0.10314100
O 1.32793900 0.06301000 -0.03756000
Al 0.00128500 -1.10918700 0.43893000
Cl -0.18184800 -1.32920700 2.65169100
C 2.78672800 2.56550400 -0.36686100
C 7.05568800 -0.24107100 -0.32507500
C -6.99180000 -0.32591000 -0.60001200
C -2.88324800 2.57913400 0.51104200
C 7.61172600 -1.67410000 -0.24373800
H 7.25083800 -2.30217000 -1.07389600
H 8.71140300 -1.64998300 -0.30081500
H 7.33981200 -2.16674500 0.70333400
C 7.64518200 0.57377000 0.84963500
H 8.74705400 0.57179700 0.80389000
H 7.31332300 1.62352500 0.82838700
H 7.34227800 0.14425600 1.81823300
C 7.51954200 0.38173600 -1.66241700
H 7.18653700 1.42610700 -1.76723800
H 8.62040600 0.37594600 -1.72729200
H 7.12380500 -0.18606700 -2.52016600
C 1.98123600 2.87499100 0.91710400
H 1.19178400 2.13428700 1.08980600
H 2.64597100 2.88635900 1.79687600
H 1.51205300 3.86996400 0.83639400
C 1.86370200 2.60812200 -1.60798100
H 1.07940800 1.84371400 -1.55076900
H 1.38072300 3.59635900 -1.68670500
H 2.44719400 2.44320200 -2.52928500
C 3.83081200 3.68758400 -0.53336200
H 4.51605400 3.75178200 0.32698000
H 4.43401800 3.56638000 -1.44735900

H 3.30882400 4.65435400 -0.61009300
C -2.14834800 2.48625100 1.86957500
H -1.72023200 3.46800700 2.13357100
H -2.84969400 2.19798800 2.67018600
H -1.33663900 1.74934900 1.84342500
C -1.90986700 3.05426500 -0.59268900
H -1.48330000 4.03551700 -0.32392800
H -1.08505400 2.34575200 -0.73146800
H -2.43900500 3.16889700 -1.55371300
C -3.97779200 3.65531800 0.65437100
H -4.53133600 3.81753200 -0.28442400
H -4.70420800 3.41027700 1.44570600
H -3.50589000 4.61253900 0.92673400
C -7.72904200 1.00729800 -0.37673100
H -7.58795500 1.39015900 0.64644100
H -7.39781300 1.78504100 -1.08306300
H -8.81011800 0.86135200 -0.52882000
C -7.55278700 -1.36021600 0.40329600
H -8.64193200 -1.47365300 0.27163300
H -7.09509100 -2.35249000 0.26635300
H -7.36515400 -1.04377800 1.44210100
C -7.28566800 -0.80275500 -2.04137100
H -6.81985100 -1.77809900 -2.25284900
H -8.37206200 -0.91121500 -2.19755500
H -6.90482900 -0.08011000 -2.78125300

S5.2.2. 1-(propylene-oxide)aminoanthraquinone (AAQ)

C -4.63797700 -1.80159500 0.01522900
C -4.26037700 -0.45981700 0.02826100
C -2.90219400 -0.10943900 0.01330400
C -1.91653500 -1.11441600 -0.01469000
C -2.30538700 -2.46220900 -0.02672800
C -3.65751200 -2.80392900 -0.01215500
C -2.51471600 1.32615400 0.03009400
C -0.45962300 -0.77974600 -0.03248700
C -0.06328900 0.63392800 -0.02632100
C -1.05443600 1.65481400 0.01300700
C -0.70390500 3.00173200 0.03944500
H -1.49480400 3.74984200 0.06958100
C 0.65111200 3.36179200 0.03540500
C 1.64504400 2.39792600 -0.00439700
C 1.32589100 1.01145400 -0.05223400
H -5.69601900 -2.07145300 0.02674700
H -5.00215200 0.33930200 0.05053400
H -1.52828300 -3.22639400 -0.04763300
H -3.95225000 -3.85545300 -0.02202700
H 0.93289400 4.41661300 0.06923700
H 2.68915100 2.70817300 0.00580700
O 0.36437700 -1.71075200 -0.04756900
O -3.36545100 2.21153200 0.05688800
N 2.30294600 0.07119900 -0.12702900
H 1.97177500 -0.89088800 -0.03320000
C 3.72842800 0.33242000 -0.05735800
H 4.04001200 0.62128600 0.96446700
H 3.99806000 1.16221700 -0.73296000
C 4.48941900 -0.89695700 -0.48679700

H 4.30524100 -1.22396800 -1.51857700
C 5.75386300 -1.28044000 0.15453100
H 6.16027000 -0.65961500 0.96159200
H 6.48972600 -1.85846900 -0.41556800
O 4.53343600 -1.97323100 0.46749900

S5.2.3. 4-Piperidinyl-(N-propylene-oxide)-1,8-naphthalimide (Nap)

O -2.3804863092 -2.3168472200 0.6172052548
C -1.9868436238 -1.1670734242 0.4481729499
N -2.8791728877 -0.0798889248 0.5827206494
C -4.2808363735 -0.3718208720 0.9299331096
C -5.2160980012 -0.2457633499 -0.2505531386
C -2.5296849444 1.2658021377 0.4287691959
O -3.3782425640 2.1428584213 0.5729416557
C -0.5918076434 -0.8344618629 0.1192469162
C -0.1705129993 0.5128444782 -0.0291209830
C -1.1197243569 1.5650516744 0.0830383769
C -0.7482534239 2.8807564135 -0.1551625898
C 0.5701818590 3.1787979814 -0.5447848667
C 1.5161418253 2.1702363355 -0.6368938485
C 1.1945937136 0.8202211803 -0.3359203096
C 2.1627207968 -0.2595509345 -0.4077609835
C 1.6825607600 -1.5764052349 -0.3290201214
C 0.3359009735 -1.8531397366 -0.0670591594
H -4.5902162722 0.3375122800 1.7102046969
H -4.3018143392 -1.3952096829 1.3176239643
H -1.5029976932 3.6626471772 -0.0650387116
H 0.8455941479 4.2060651368 -0.7897859236
H 2.5207487818 2.4142630025 -0.9794400716
N 3.5091934545 0.0204434589 -0.6047798935
H 2.3771540116 -2.4112596626 -0.4083120687
H 0.0005435614 -2.8863650886 0.0329884812
C 4.2332214634 0.9470146112 0.2864719460
C 4.3971525666 -0.9717590856 -1.2245655275
C 5.0551692960 0.1953655159 1.3458924679
H 3.5177532610 1.6145589592 0.7784691409
H 4.9045777182 1.5731827309 -0.3303301869
C 5.2326943637 -1.7723919196 -0.2153625262
H 5.0847470157 -0.4112253019 -1.8856210305
H 3.8009824128 -1.6270248026 -1.8732330661
C 6.0069335425 -0.8218968146 0.7067261737
H 5.9218342802 -2.4361294461 -0.7638262942
H 4.5729616768 -2.4199670195 0.3883243502
H 6.7734083634 -0.2849423365 0.1167849605
H 6.5462050706 -1.3882599351 1.4832903455
H 4.3627358229 -0.3216333902 2.0342823285
H 5.6149699734 0.9326697019 1.9458100060
C -6.3898492397 -1.1229904439 -0.3750956090
O -5.2252841577 -1.3349576718 -1.1887200371
H -7.2785319804 -0.7617506548 -0.9056193854
H -6.5729298426 -1.8892800316 0.3878014871
H -5.2577292453 0.7468185017 -0.7130821106

S6. Chemical recycling studies

S6.1. Depolymerization and monomer reformation procedures

The naphthalimide-doped polymer [Nap-PA-CHO] (1.0 g, 1.29 mmol) was dissolved in THF (180 mL) and a 40% w/v solution of potassium hydroxide (20 mL) was added. The resulting solution was stirred and heated to 90 °C for 3 days. After cooling, the solution was concentrated under reduced pressure and cooled overnight at -20 °C. The organic layer was separated and dried ($MgSO_4$) followed by evaporation of the solvent to yield a mixture of *trans*-1,2-cyclohexanediol and 4-piperidinyl-(N-propane-2,3-diol)-1,8-naphthalimide as a yellow solid. The presence of the naphthalimide component was confirmed by high-resolution electrospray mass spectrometry (ES-MS): found *m/z* = 377.1481; calculated for $C_{20}H_{22}N_2O_4Na$ *m/z* = 377.1477 ($[M+Na]^+$, 0.4 ppm deviation). *Trans*-1,2-cyclohexanediol was purified via recrystallization from ethyl acetate at -20 °C, from which single crystals were grown and the structure verified by X-ray diffraction (See section S2.4). An aliquot was taken from the aqueous layer, concentrated under reduced pressure, and subsequently left overnight to afford potassium phthalate as a white precipitate.

S6.1.1. Phthalic anhydride reformation:

Acetic anhydride (340 mmol, 37.5 mL, 5.6 eq) was added to a solution of *recycled*-phthalic acid (60 mmol, 10g, 1 eq) dissolved in chloroform (125 mL) and heated at reflux for 2 h. Phthalic anhydride precipitated as a white solid upon cooling and was collected by filtration. The filtrate was concentrated *in vacuo*, resulting in more phthalic anhydride precipitation and subsequent isolation by filtration. All product was combined and sublimed under high vacuum at 110 °C (5.16 g, 58%). ^{1}H NMR (300 MHz, DMSO) δ 8.13 – 8.05 (m, 2H, CH), 8.05 – 7.97 (m, 2H, CH).

S6.1.2. Cyclohexene oxide reformation:

A solution of diethyl azodicarboxylate (40% in Toluene) (13.64 mL) was added dropwise over 4 h to a suspension of *recycled*-cyclohexane diol (30 mmol, 3.48 g, 1 eq.) and triphenylphosphine (30 mmol, 7.68 g, 1eq.) in diethyl ether (60 mL). After stirring overnight, a white precipitate was removed by filtration and the solvent was removed *in vacuo* to give a yellow solution. The filtrate was then distilled under vacuum at ambient temperature to afford cyclohexene oxide. The product was subsequently dried over calcium hydride, isolated *via* trap-to-trap distillation and stored in a glovebox under Nitrogen atmosphere. (Yield: 33% by ^{1}H NMR against 1,4-dimethoxybenzene internal standard, isolated 761 mg, 25%). ^{1}H NMR (300 MHz, $CDCl_3$) δ 3.09 – 3.01 (m, 2H, CH), 1.95 – 1.81 (m, 2H, CH_2), 1.81 – 1.66 (m, 2H, CH_2), 1.44 – 1.27 (m, 2H, CH_2), 1.26 – 1.06 (m, 2H, CH_2).

S6.2. UV Concentrations:

Crude Diols: 1mg/mL in Chloroform
Recrystalized Cyclohexanediol: 1mg/mL in Chloroform
Mother Liquor: 1mL of supernatant in 5mL EtOAc

S6.3. Mass spectrum of potassium phthalate in water (ES in negative ion mode)

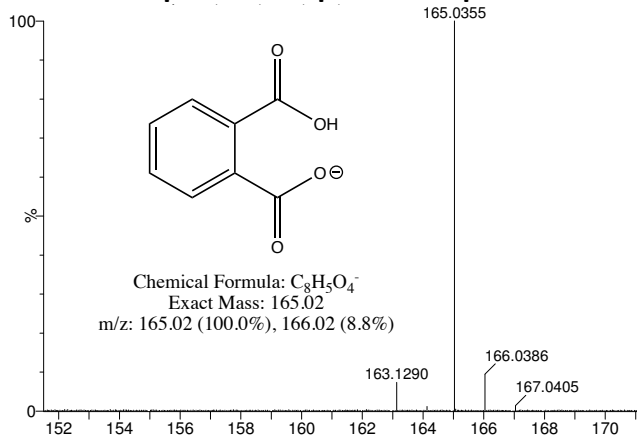

S6.4. ^{1}H NMR spectrum of recrystallized *trans*-1,2-cyclohexane diol

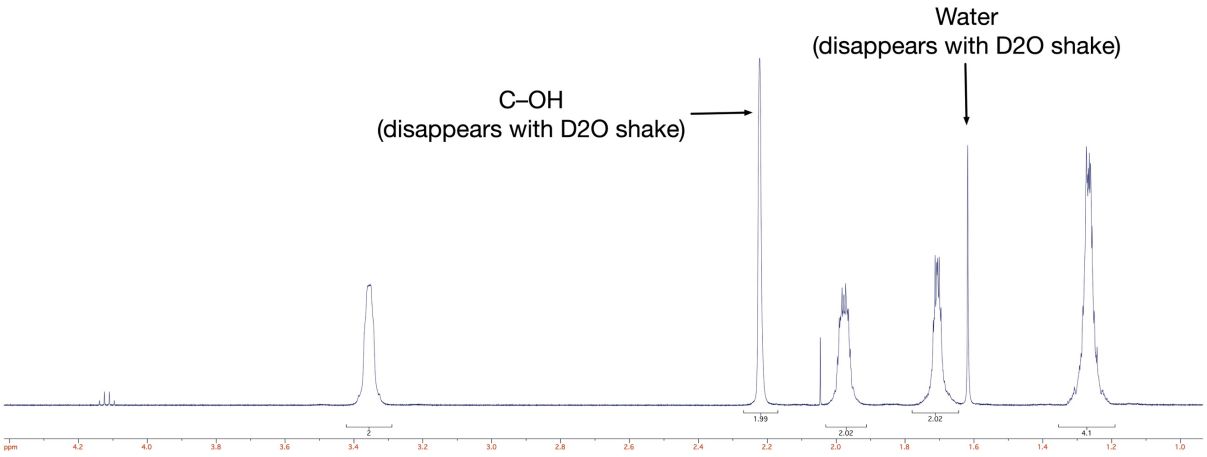

S6.5. ^{1}H NMR spectrum (500 MHz, $CDCl_3$) of PA-CHO remade from recycled Nap-PA-CHO.

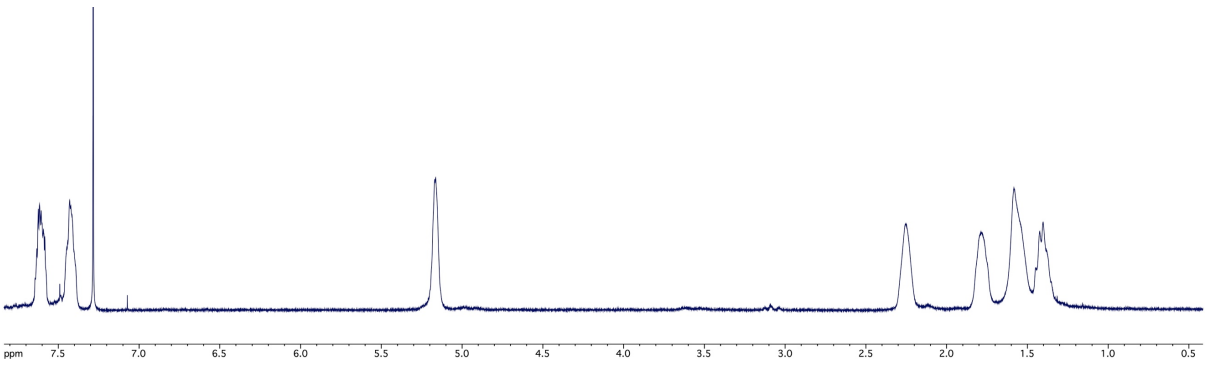

S6.6 Photograph of Nap-PA-CHO and remade PA-CHO

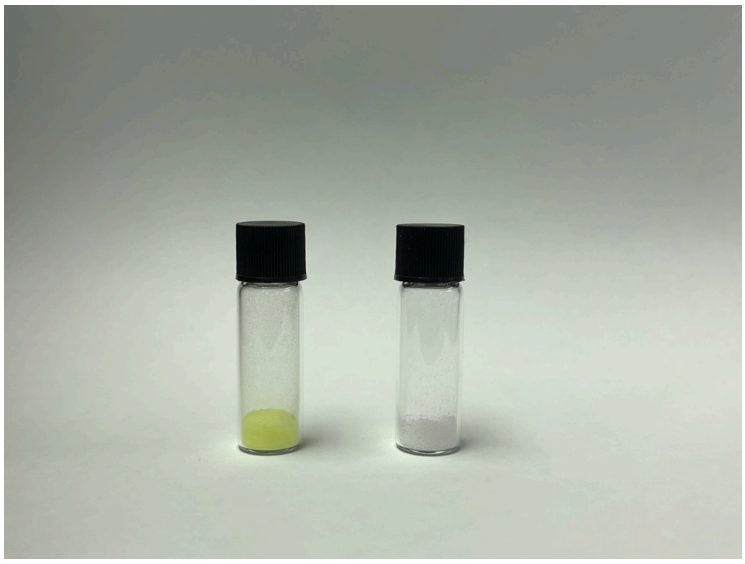

S7. References

(1) Rutherford, D.; Atwood, D. A. Five-Coordinate Aluminum Amides. *Organometallics* **1996**, *15* (21), 4417–4422. https://doi.org/10.1021/om9603631.

(2) Chi P.; Xie C.; Lin J. A Novel Synthetic Method of 5-Aminolevulinic Acid Hydrochloride. *Chin. J. Org. Chem.* **2013**, *33* (3), 640–642. https://doi.org/10.6023/cjoc201210005.

(3) Getautis, V.; Dashkyavichene, M.; Paulauskaite, I.; Stanisauskaite, A. Study of the Products from Reaction of 1(2)-Aminoanthraquinones with 1-Chloro-2,3-Epoxypropane. *Chem. Heterocyc. Comp.* **2005**, *41*, 426–436.

(4) Han, B.; Zhang, L.; Liu, B.; Dong, X.; Kim, I.; Duan, Z.; Theato, P. Controllable Synthesis of Stereoregular Polyesters by Organocatalytic Alternating Copolymerizations of Cyclohexene Oxide and Norbornene Anhydrides. *Macromolecules* **2015**, *48* (11), 3431–3437. https://doi.org/10.1021/acs.macromol.5b00555.

(5) Van Zee, N. J.; Coates, G. W. Alternating Copolymerization of Propylene Oxide with Biorenewable Terpene-Based Cyclic Anhydrides: A Sustainable Route to Aliphatic Polyesters with High Glass Transition Temperatures. *Angew. Chem. Int. Ed.* **2015**, *54* (9), 2665–2668. https://doi.org/10.1002/anie.201410641.

(6) Saini, P. K.; Romain, C.; Zhu, Y.; Williams, C. K. Di-Magnesium and Zinc Catalysts for the Copolymerization of Phthalic Anhydride and Cyclohexene Oxide. *Polym. Chem.* **2014**, *5* (20), 6068–6075. https://doi.org/10.1039/C4PY00748D.

(7) Coles, S. J.; Gale, P. A. Changing and Challenging Times for Service Crystallography. *Chem. Sci.* **2012**, *3*, 683–689.

(8) Dolomanov, O. V.; Bourhis, L. J.; Gildea, R. J.; Howard, J. A. K.; Puschmann, H. *OLEX2* : A Complete Structure Solution, Refinement and Analysis Program. *J Appl Crystallogr* **2009**, *42* (2), 339–341. https://doi.org/10.1107/S0021889808042726.

(9) Sheldrick, G. M. A Short History of SHELX. *Acta Cryst.* **2008**, *A64*, 112. https://doi.org/10.1107/S0108767307043930.

(10) Sheldrick, G. M. SHELXT – Integrated Space-Group and Crystal-Structure Determination. *Acta Cryst.* **2015**, *A71* (1), 3–8. https://doi.org/10.1107/S2053273314026370.

(11) Sheldrick, G. M. Crystal Structure Refinement with SHELXL. *Acta Cryst.* **2015**, *C71* (1), 3–8. https://doi.org/10.1107/S2053229614024218.

(12) Frisch, M. J.; Trucks, G. W.; Schlegel, H. B.; Scuseria, G. E.; Robb, M. A.; Cheeseman, J. R.; Scalmani, G.; Barone, V.; Mennucci, B.; Petersson, G. A.; Nakatsuji, H.; Caricato, M.; Li, X.; Hratchian, H. P.; Izmaylov, A. F.; Bloino, J.; Zheng, G.; Sonnenberg, J. L.; Hada, M.; Ehara, M.; Toyota, K.; Fukuda, R.; Hasegawa, J.; Ishida, M.; Nakajima, T.; Honda, Y.; Kitao, O.; Nakai, H.; Vreven, T.; Montgomery Jr, J. A.; Peralta, J. E.; Ogliaro, F.; Bearpark, M.; Heyd, J. J.; Brothers, E.; Kudin, K. N.; Staroverov, V. N.; Keith, T.; Kobayashi, R.; Normand, J.; Raghavachari, K.; Rendell, A.; Burant, J. C.; Iyengar, S. S.; Tomasi, J.; Cossi, M.; Rega, N.; Millam, J. M.; Klene, M.; Knox, J. E.; Cross, J. B.; Bakken, V.; Adamo, C.; Jaramillo, J.; Gomperts, R.; Stratmann, R. E.; Yazyev, O.; Austin, A. J.; Cammi, R.; Pomelli, C.; Ochterski, J. W.; Martin, R. L.; Morokuma, K.; Zakrzewski, V. G.; Voth, G. A.; Salvador, P.; Dannenberg, J. J.; Dapprich, S.; Daniels, A. D.; Farkas, O.; Foresman, J. B.; Ortiz, J. V.; Cioslowski, J.; Fox, D. J. Gaussian 09, Revision D.01, 2010.